2012

Biodegradation Study of Polymeric Material with Various Levels of Molecular Orientation Induced via Vibration-Assisted Injection Molding

Qi Li
Lehigh University

Biodegradation Study of Polymeric Material with Various Levels of Molecular Orientation Induced via Vibration-Assisted Injection Molding

Qi Li

Presented to the Graduate and Research Committee

of Lehigh University

in Candidacy for the Degree of

Master of Science

in

Mechanical Engineering and Mechanics

Lehigh University

Bethlehem, Pennsylvania

January 2011

CERTIFICATE OF APPROVAL

Thesis is accepted and approved in partial fulfillment of the requirements for the Master of Science in Mechanical Engineering and Mechanics.

Biodegradation Study of Polymeric Material with Various Levels of Molecular Orientation Induced via Vibration-Assisted Injection Molding

Qi Li

_____

Date

_____

Dr. John P. Coulter

Dissertation Advisor and Committee Chairman Associate Dean of P.C. Rossin College of Engineering

Department of Mechanical Engineering and Mechanics

_____

Dr. Gary Harlow

Department Chair

Mechanical Engineering and Mechanics

Table of Contents

List of Tables

List of Figures

ABSTRACT

Vibration-Assisted Injection Molding (VAIM) has been a remarkable technology, which can be used for changing the morphology inside polymer devices. One such characteristic is known as molecular orientation. The molecular orientation of a polymer sample can be enhanced in a direction parallel to the molding flow or the vibration direction. By applying different vibration frequencies or vibration durations, this enhancement can be achieved and the birefringent patterns of this enhancement can be observed under cross-polarization. Generally speaking, increased degree of molecular orientation can be realized by increasing the vibration frequency and vibration duration.

Applying the Vibration-Assisted Injection Molding technology, a research study focused on whether different levels of molecular orientation could affect the biodegradation rate of polymeric material was carried out. In this study, several chemical, thermal and mechanical tests were performed in order to monitor the biodegradation behavior of PLA samples, which were conventionally molded and VAIM molded separately.

The PLA samples were made and classified into three groups: conventional, VAIM_Low and VAIM_High with no molecular orientation, low levels of molecular orientation and high levels of molecular orientation respectively. GPC, FT-IR, DSC, TGA, weight measurement and tensile test were applied in this research. Though no significant changes in weight resulted during the timeframe of the study, there were still some persuasive results obtained from other tests denoting that the modified molecular orientation could influence the biodegradation manner of PLA specimens. Based on this investigation, it appears that specimens with higher levels of molecular orientation have an enhanced tensile strength along the orientation direction and these samples are more resistant to hydrolysis, indicating a slower biodegradation rate.

Chapter 1: Introduction

1.1 Problem Description

One of the critical issues in surgery regarding implants or sutures is the removal of the implants or suture strings after recovery. This issue needs a second procedure to recover the part, which could cause a secondary wound or infection. In this case, not only does it take a longer time for the patient to fully recover, but it also increases the risk of operation and infection. Even for the extended time implants, failures can result, such as rupture, deformation or phase change. These can be caused by aging, the application of complex loads, erosion or hydrolysis and environmental factors inside human body.

Another critical complication of a medical implant is the biocompatibility. So far as we know, not all of the medical implant devices we are using today are completely biocompatible. Our human body is a complicated system which is so sensitive that it can identify the particles or devices not generated by our body, and start the rejection reaction. In a healthy body, once some unknown or external elements, like tiny rocks, cells from other bodies, viruses, bacteria or even food, are detected, the body will clean out or change them into other compatible elements to keep the body clean, pure and healthy. In this situation, the implant devices will have to face the risk of any rejection reaction. However, the acuteness of rejection reaction is dependent. The implants which lead to relatively slow and little rejection reaction are acceptable in the medical arena. So some materials, which are called biocompatible materials, accord with this acceptability and can be used as implant device materials.

Biocompatible materials can be either organic or inorganic, like polymeric products, silica gels and magnesium alloys. Some of these materials are also biodegradable.

Biodegradable materials can degrade completely inside the human body, leaving non-toxic by products to be purged or digested by the body circulatory system. By using biodegradable and biocompatible materials to produce the implant devices, the implants can degrade during the recovery of the wounded area. This will obviate the original second operation of removing the implant later to reduce unnecessary risks caused by the implant itself.

Although the biodegradable materials have some advantages, there is still one uncertainty left to be considered: the degradation rate. Take the use of biodegradable implants as an example. Different biodegradable materials have different biodegradation rates. The degradation rate of polymeric implants also depends on the location in the body. For replacement of bone structure or bone segments, the degradation rate of the implant can be different if it is placed in the head, arm, hip, leg or toes. Because the environment surrounding the polymer is different depending on the location in the body, the recovery speed of bones in these places can be different. So it follows that the biodegradation rate of the implant should meet with the recovery process in each specific degradation environment, which means that these biodegradable materials should have the property of controllable degradation rate. Also, the stiffness, toughness and the ease of manufacture of the implants in various conditions are not insignificant.

1.2 Potential Solution

Many recent research efforts have been aimed at finding ways to control the degradation rate. Some of these have been successful, such as adding coating materials to the original material, blending different materials together, changing the cross-link level of cross-linked polymers, increasing the crystallinity or using some other methods of polymerization for polymeric materials.

Magnesium alloys are one of the biocompatible and fast degrading materials. It can be fully degraded within a month when placed into SBF (Simulated Body Fluid). A polymer coating added to Mg alloys can help to increase the resistance ability against degradation and slow down the degrading rate.

For polymeric materials, simply by blending different polymers at different ratios, many levels of crystallinity can be achieved, because samples with more amorphous regions are easier to degrade. Some other ways, as changing the molecular weight of polymer and adding enzymes to the degrading circumstance, many also affect the biodegradation speed.

1.3 Research Objectives and Approach

There are many kinds of polymers which degrade at different rates. Even for one type of polymer, the degradation speed depends on the testing conditions, processing factors and polymer blending. In this research, Polylactic acid(PLA) was the main mentioned testing material.

This research was mainly aimed at changing the molecular orientation of the polymer itself in order to achieve specific degradation rates. From the previous researches, it was partially proved that a higher degree of molecular orientation increases the resistance of polymers against degradation by applying weight measurement, tensile test, Fourier Transform Infrared Spectroscopy (FT-IR), Differential Scanning Calorimetry (DSC) and Thermogravimetric Analysis(TGA). In this study, weight measurement in a dried condition and Gel Permeation Chromatography (GPC), together with the tests mentioned above, were included to verify the molecular orientation effect on biodegradation rate. Moreover, the effect of enzymes in the degradation environment was also taken into consideration.

The vibration-assisted injection molding (VAIM) technique was investigated in controlling the molecular orientation levels. In this way, the biodegradation level or rate could be controlled indirectly and it would be much easier than some of the original manufacturing methods proposed. A Nissei PS-40 injection molding machine was used to perform VAIM, using a variety of vibration duration and vibration frequency values.

1.4 Structure of the Thesis

In chapter 2, biodegradation and VAIM will be explained in detail. The original concept, phenomenon, physical changes, chemical reactions and phases associated with biodegradation will be indicated. A distinction between bulk erosion and surface erosion will be made. Some kinds of biodegradable plastics

and polymers together with their properties will be discussed. The utility of injection molding and Vibration-Assisted Injection Molding will also be highlighted. Also the brief historical studies of both biodegradation and VAIM will be mentioned. Chapter 3 will give the exact manufacturing plan to make samples by Vibration-Assisted Injection Molding and the necessary process after that. The desired shape and dimensions according to standards will be explained. Similarity and differences between molecular orientation and crystallinity will be clarified. Parameters of each type of specimens, conventionally made, VAIM low, VAIM moderate and VAIM high, will be illustrated and how they affect the levels of molecular orientation will be included.

Chapter 4 will provide the tests applied to investigate the biodegradation. It will describe the preparation of the samples before testing and the six main tests individually. Protocols of degradation solution, enzyme and incubation will be listed as well. Chapter 5 will then analyze and present the experimental results and discussions. All conclusions from the gained results and discussions will be presented in Chapter 6. The recommendations for future research, which will be based on the current study or may be deeper and further than this investigation, will also be given in this chapter.

Chapter 2: Related Scientific Background

2.1 Biodegradable Polymers

2.1.1 Biodegradation

Biodegradation is a kind of progression of events during which materials are dissolved chemically by bacteria or some other biological ways. Most biodegradable matter consists of organic materials generated from plants, animals or artificial substances which are similar enough to plant and animal matter.

Biodegradation progression can be carried out with or without enzymes. Two typical kinds of general biodegradation without enzyme are surface erosion and bulk erosion (Figure 2.1).

All degradable polymers share the property of eroding upon degradation. Degradation or erosion are the decisive performance parameters of biodegradable materials. So another way to classify degradable polymers is using a distinction made between surface eroding material and bulk eroding material. [1]

During an application, surface eroding polymers lose material from the surface only. Surface eroding polymers do not allow water to penetrate into the material. They erode layer by layer, like a lollipop. They get smaller but keep their original geometric shape. For bulk eroding polymers, degradation and erosion are not confined to the surface of the device. Bulk eroding polymers take in water like a sponge (throughout the material) and erode both inside and on the surface of the polymer. Therefore, the size of a device will remain constant for a considerable portion of time during its application. [2] (Figure 2.1) The surface eroding polymers have some advantages, one of which is the predictability of the

erosion process. [3] To use this particular advantage, such polymers can be used for drug delivery as the release of drugs can be related directly to the rate of polymer erosion. [4] Surface and bulk erosion are ideal cases to which most polymers cannot be unequivocally classified.

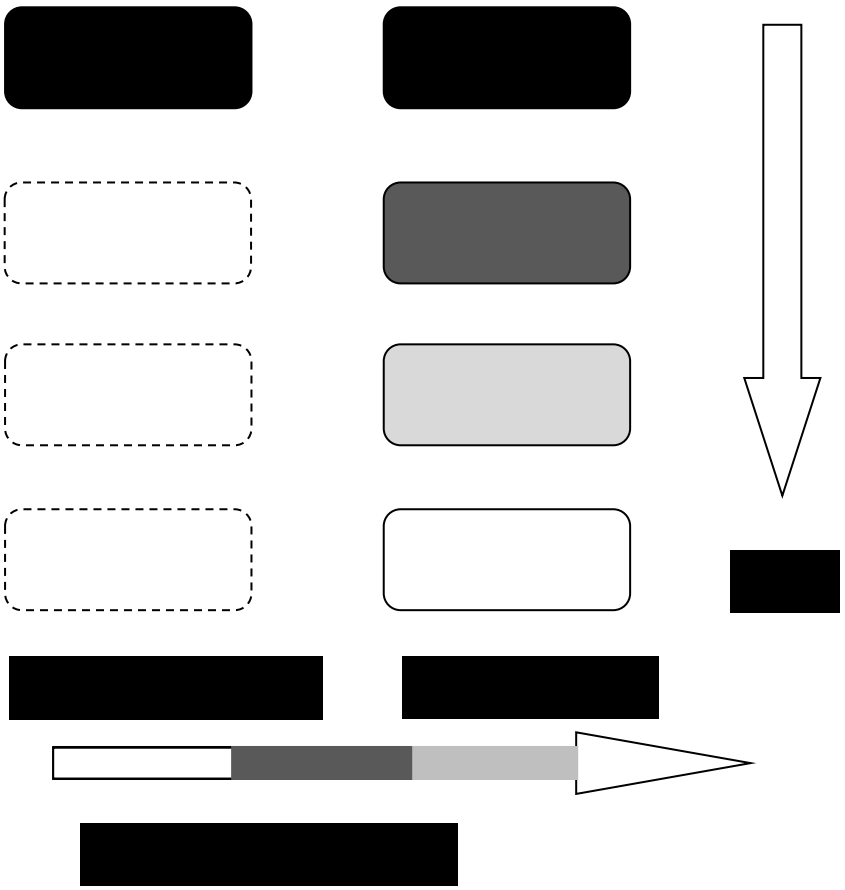

Figure 2.1: Surface and bulk erosion

Almost all polymers and polymeric devices share the same phases of degradation. During the first phase of degradation, the biodegradable sample is penetrated by water. Initially, the water breaks down the chemical bonds and converts the long chain like polymers into shorter ones. This step is called hydrolysis. In the second phase, the shorter polymers are degraded into natural

monomeric acids which can be found in our human body, such as lactic acid. Then these acids are metabolized into carbon dioxide and water which are excreted in the third phase.

Many different indicators during degradation have been proposed, such as molecular weight loss, sample weight loss and changes of geometry. These parameters do not change at the same rate as the example of poly(anhydrides) illustrates. The loss of molecular weight can be dominant during the first 12 h [5], while there is almost no loss of weight and no change in geometry. [6] Also, the degradation rate of different polymers can individually differ from each other.

The factors which control the rate of degradation include percentage of crystallinity or the microstructure, molecular weight and hydrophobicity.

The crystallinity refers to whether it is amorphous or crystalline. (Figure 2.2) In an amorphous structure, the polymer chains are oriented very randomly or loosely packed. The chains can slip past each other easily. For crystalline polymers, they have areas or regions in which the chains lie parallel and close to each other. [7]

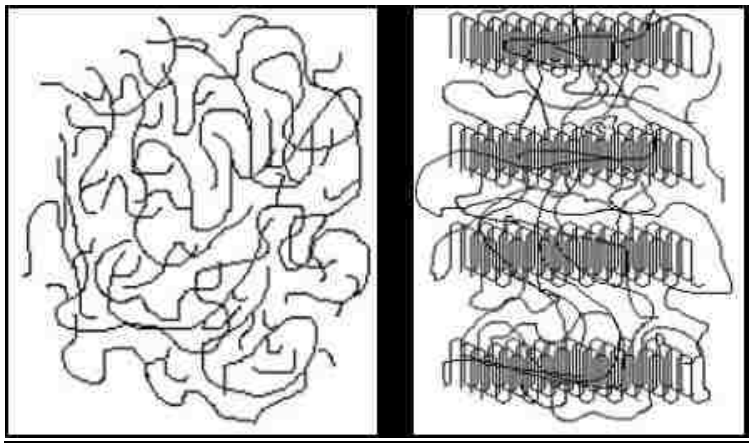

Figure 2.2: Amorphous and semi-crystalline polymer with crystalline and amorphous regions [7]

However, even crystalline polymers are never completely crystalline. In fact, crystalline polymers always contain both crystalline and amorphous regions. Therefore, they are better termed semi-crystalline. (Figure 2.2)

Amorphous polymers have random structures and they are more easily degraded. In contrast, the internal structures in crystalline polymers are more regular and because of this, crystalline polymers degrade slowly. As for semi-crystalline polymers, they have both kinds of regions. Degradation of the implant begins from the amorphous region. [7]

Some other artificial elements can affect the biodegradation rate as well. Like the molecular orientation inside the polymer sample, shape of the implant, surface area, solutions in which the samples are stored, temperature of the degradation environment and with or without enzymes.

2.1.2 Biodegradable Plastics and Biodegradable Polymers

Biodegradable materials can be derived from natural resourses or raw materials, like starch, corn, sugar cane or petroleum. Polyanhydrides, Polyvinyl alcohol and most of the starch derivatives are examples of biodegradable plastics. Poly-3-hydroxybutyrate (PHB), polyhydroxyvalerate (PHV) and polyhydroxyhexanoate (PHH) are polyhydroxyalkanoates (PHAs) which can be naturally produced. Polylactic acid (PLA) is a renewable resource. Polybutylene succinate (PBS) and polycaprolactone (PCL) are synthetic materials. Hyperbranched poly(ester-amide) (HBP) is made from agricultural resources such as corn, wheat, sugar cane, or fossil (petroleum-based)resources , or blend of the

two. Due to the potentially hydrolysable ester bonds, most aliphatic polyesters are biodegradable.

There are two typical ways to produce products from biodegradable plastics. One is injection molding which is typically used in producing disposable food service items. The other is filming which is typically utilized in producing organic fruit packages or agricultural mulch.

2.1.3 History and Application

When talking about biodegradation, people often relate it to ecology, environmental issues or biomedical materials. Nowadays, it is commonly combined with environmentally friendly products which are able to decompose back into natural elements. During the past few years, the market for biodegradable material has been growing rapidly.

The words, biodegradable or biodegradation, were first known in biological text in 1961, when it was used to describe a material that was able to break down into basic components , such as carbon, oxygen and hydrogen.

The use of biodegradable polymers can be traced back to the times of the Romans. One of the desired properties was that it slowly degrades after a suture as the wound heals. Cat gut was used as this kind of material, but it caused some froms of inflammatory responses.

As biodegradable polymers can break down and lose their initial integrity, in the last two decades the use of biodegradable materials has expanded to include

fixation applications and been used in medical devices to gradually release a drug, or to avoid a second operation to remove them. [8]

For drug release or drug delivery, the polymer slowly degrades into smaller fragments with a controlled ability, releasing a natural product into the environment.

Besides sutures and controlled drug release, biodegradable polymers also have been used in tissue engineering. For examples, a porose cup can be used to create organs, such as the kidney from basic constituents. A polymer scaffold can also be placed in blood vessels to create enough space for circulation or somewhere else inside human the body to help grow some entity into a functional organ. All these scaffolds should be dissolvable and biocompatible. Another main attraction of a biodegradable device, to both surgeons and patients, is that it provides the desired amount of strength when implanted for bone surgery or replacement over time of degradation, until the load can be safely transferred to the healed bone. As the traditional operation to remove the implant is often required once the healing process is complete if a metal device were used, by using biodegradable material, there is no need for an additional, removal operation. In this way, reducing the total treatment and rehabilitation time of the patient can be achieved. There are also obvious economical advantages to avoiding an expensive removal operation for both patients and surgeons. [7]

2.1.4 Polymers Studied

Biodegradable polymers in studies should have some properties worthy of investigation. First of all, they should be non-toxic. Secondly, they should be able to maintain good mechanical integrity until getting degraded to some degree. They also should be capable of controlled rates of biodegradation.

In this research, the biodegradable material is PLA. PLA is short for Poly(lactic acid). It is a biodegradable, thermoplastic, aliphatic polyester which is derived from renewable resources.

PLA is widely used in biomedical and industrial applications, as a material for tissue engineering or being employed in the preparation of bio-plastic products, which will be useful to produce food packaging or disposable tableware.

PLA biodegradation is mainly about hydrolysis of ester bonds. Figure 2.3 shows the skeletal formula of PLA and there are many ester linkages in it (Figure 2.4).

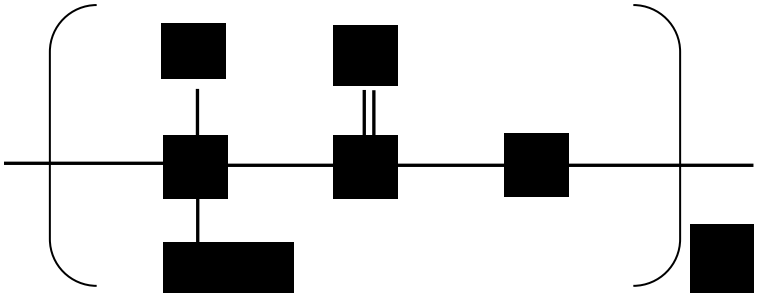

Figure 2.3: Formulas of PLA

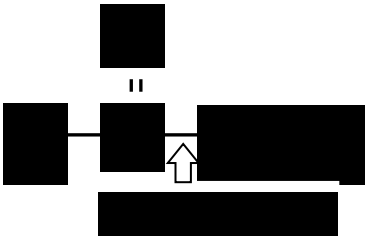

Figure 2.4: Ester bond or ester linkage

In PLA hydrolysis, a water molecule penetrate into the product, cleaves the ester bond and splits itself into H+ and OH-, creating a new carboxyl end group. (Figure 2.5 and Figure 2.6)

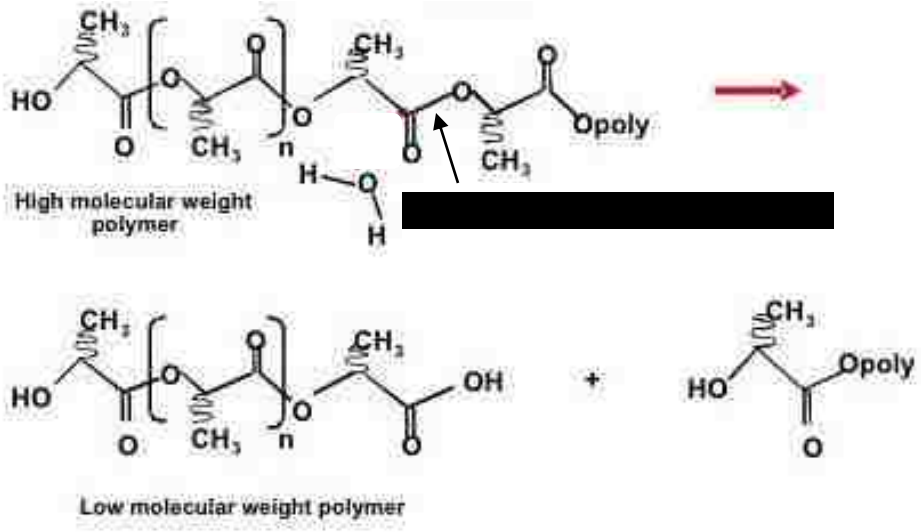

Figure 2.5: Hydrolysis and cleavage of the ester linkage [9]

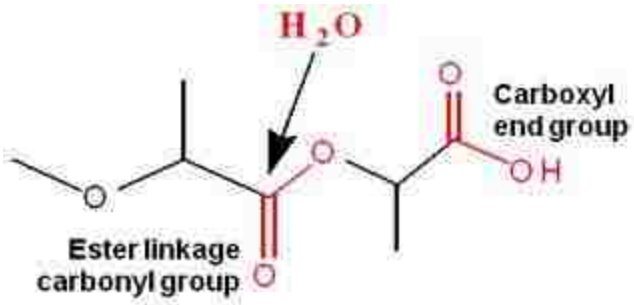

Figure 2.6: Carboxyl end group [10]

As we can see from the figures that hydrolysis not only decreases molecular weight, but also decreases the amount of ester bonds and increases the concentration of carboxyl end group.

The PLA materials used during the study were PLA 3051D and 3052D, provided by NatureWorks LLC. 3051D is composed of 96% of L-Lactide and 4%

of D-Lactide units. PLA 3052D is a new generation of product similar to PLA 3051D. NatureWorks LLC started to provide PLA 3052D instead of PLA 3051D, which is not produced any more since 2011.

When dilactide is prepared from racemic lactic acid, the three isomers that result are D-lactide, L-lactide and meso- lactide. (Figure 2.7)

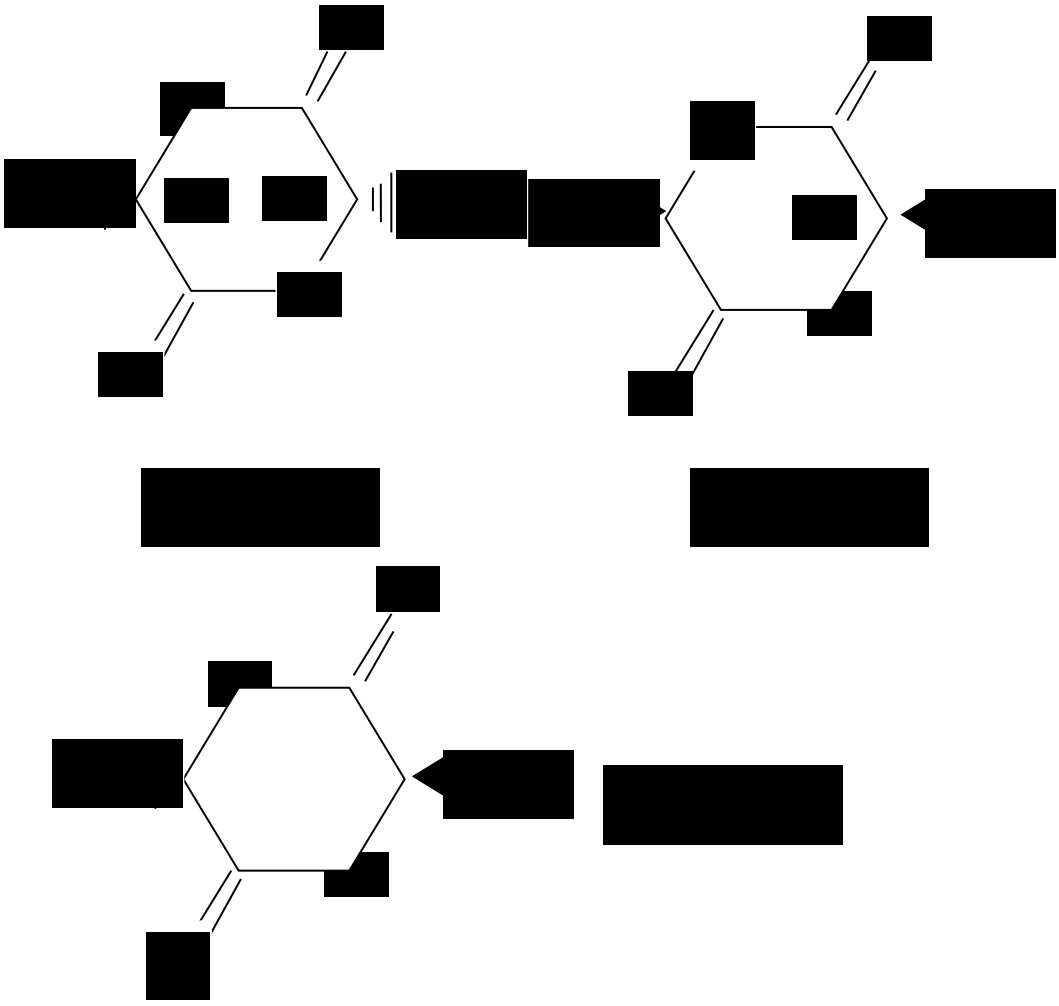

Figure 2.7: L-lactide D-lactide and meso-lactide (The meso isomer can be removed)

A mixture of L-lactide and D-lactide is polymerized, leading to the synthesis of poly-DL-lactide (PDLLA) which is more amorphous like. The degree

of crystallinity, and hence many other important properties, is largely depending on the ratio of D to L enantiomers used.

Biodegradation of pure or high volume fraction of PDLA is slower than that of PLLA due to the higher crystallinity of PDLA. So in this study, PLA 3051D and 3052D were chosen to expecting relatively faster degradation.

2.2 Injection Molding

2.2.1 History and Applications

Injection molding, which is ideal for producing high volumes of the same object, is one of the most popular manufacturing processes in the modern world. Both thermoplastic and thermosetting materials can be used in injection molding.

American inventor John Wesley Hyatt together with his brother Isaiah, patented the first injection molding machine in 1872. Nowadays, injection molding is commonly used to create many things like wire spools, bottle caps, automotive dashboards, pocket combs, and most other plastic products (Figure 2.8).

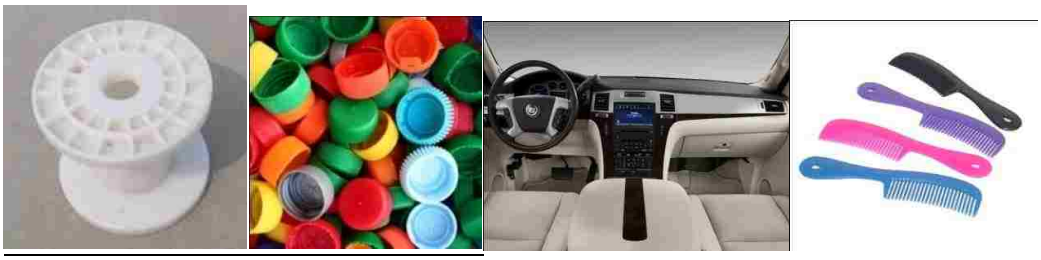

Figure 2.8: Products made by injection molding [11]

So injection molding has some advantages such as a fast speed of producing, repeatable high tolerances, the ability to use a wide range of materials, low labor cost, minimal scrap loss and little need to finish parts after molding.

Injection molding machines consist of a injection unit which includes material hopper, an injection ram, and a clamping unit. (Figure 2.9 and Figure 2.10)

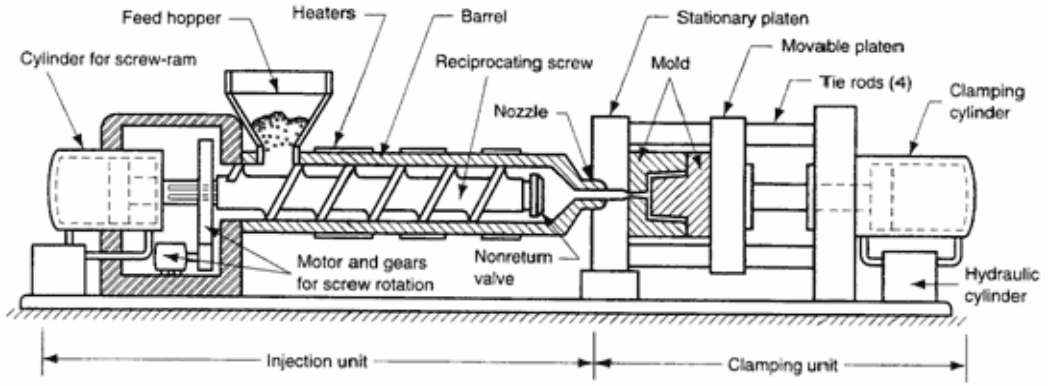

Figure 2.9: Composition of injection molding machine [12]

Figure 2.10: Injection molding equipment used in this study

Figure 2.11 shows the injection molding cycle. The cycle begins when the mold closes, followed by the injection of the polymer into the mold cavity. Once the cavity is filled, a packing pressure is maintained to compensate for material

shrinkage. In the next step, the screw turns, feeding the next shot to the front screw. This causes the screw to retract as the next shot is prepared. Once the part is sufficiently cool, the mold opens and the part is ejected.

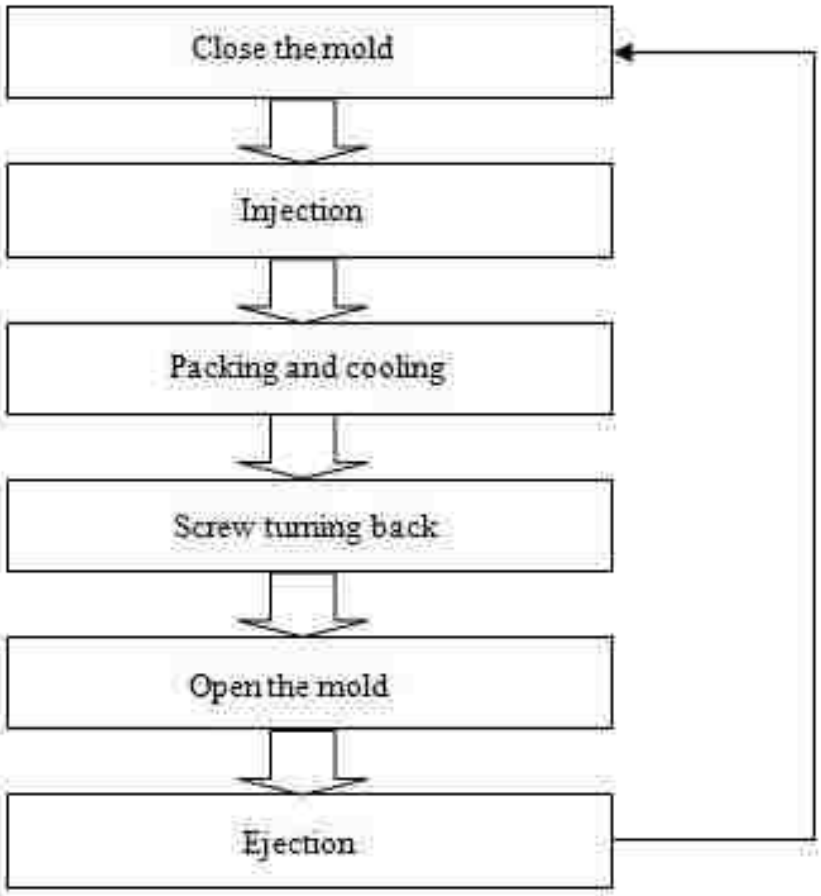

Figure 2.11: Injection molding cycle

2.2.2 VAIM

Vibration-Assisted Injection Molding is also known as a dynamic melt manipulation technique. It is used to achieve modified molecular orientation level in injected molded parts.

During injection molding, an additional oscillatory energy is imposed on the molten polymer flow, causing the long chain-like molecules to align parallel to the flow direction. These orientations can be locked in to the final product. (Figure 2.12)

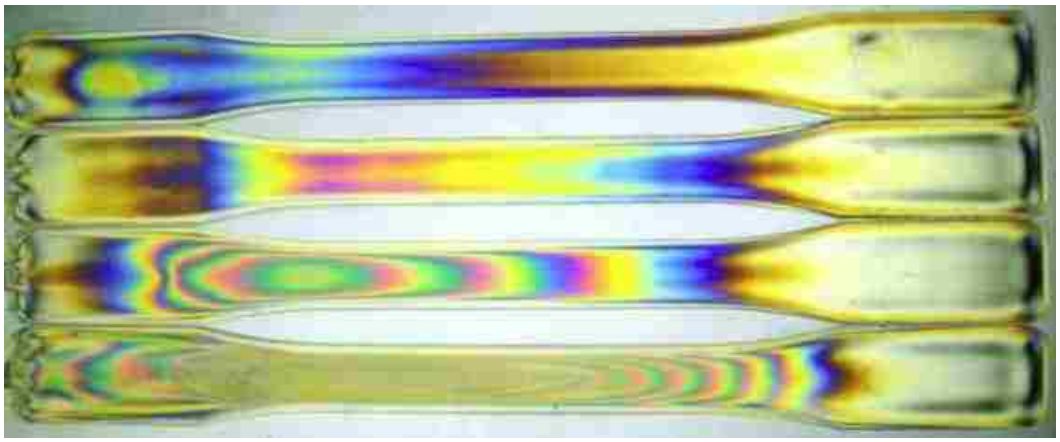

Figure 2.12 Different orientation levels in parts

A computer is simply used to turn two directional flow valves on and off to apply compression or decompression at an alternating order and at a defined frequency. (Figure 2.13)

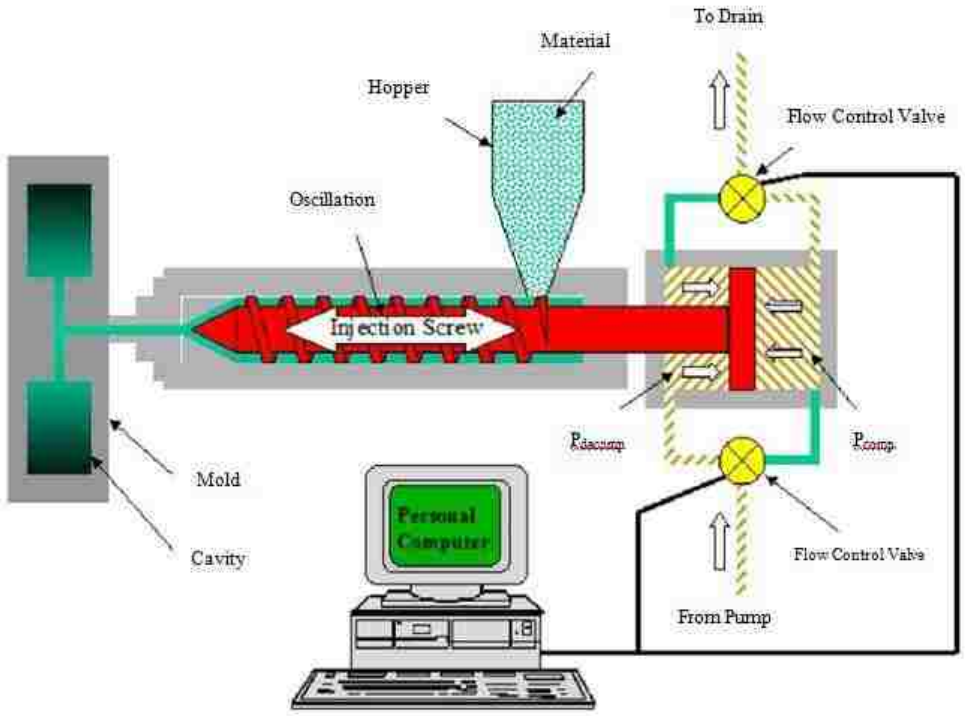

Figure 2.13: Control of vibration assisted injection molding [13]

2.2.3 Previous Studies with VAIM

Previous works have been done to prove that by applying VAIM, some properties of samples had been changed systematically.

By using VAIM, the molecular orientation level can be altered. (Figure 2.12) During the vibration duration, short duration leads to high degree of relaxation when the material solidifies in the mold cavities, so the molecular orientation, as evidenced by the birefringence, tends to be lower. In long duration, there is less relaxation during packing and a high degree of orientation is evident. [14]

For tensile investigation on different polymers, the ultimate tensile strength (UTS) was increased on samples which were produced by using VAIM.

Polystyrene and its copolymers were the most popular materials studied during the past few years. Table 2.1 shows that the best VAIM trial on pure polystyrene produced a 15.9% increase in the average UTS. [14]

	UTS (MPa)		
	Av'g	Δ%	Std. Dev.
CONV	42.6	---	0.96
V2	49.3	15.9%	1.12
V5	49.2	15.6%	2.11
V6	48.9	14.8%	0.69
V8	48.1	12.9%	0.84
V9	47.1	10.7%	1.33
V1	46.9	10.2%	0.73
V4	46.6	9.5%	1.36
V7	45.1	5.9%	1.83
V3	44.6	4.7%	1.81

Table 2.1: Average UTS for conventionally molded and VAIM produced polystyrene samples listed in order from highest average UTS to lowest. [14] (V# means VAIM produced samples)

For Polystyrene / Styrene-Acrylonitrile Copolymer, the UTS increase attained was 11.2%. The overall average UTS for all runs were 69.3 MPa with a minimum of 67.0 MPa and a max of 71.9 MPa. (Table 2.2) This compares to 64.4 MPa, the average UTS for the conventionally molded samples. [14]

	UTS (MPa)		
	Av'g	Δ%	Std. Dev.
CONV	64.6	---	0.88
V6	71.9	11.2%	1.07
V2	71.2	10.2%	0.52
V7	70.2	8.6%	0.56
V9	69.6	7.6%	0.72
V5	69.0	6.8%	1.14
V8	68.5	6.0%	0.74
V3	68.0	5.2%	0.68
V1	67.8	4.8%	0.92
V4	67.0	3.7%	1.63

Table 2.2: Average UTS for conventionally molded and VAIM produced Polystyrene / Styrene-Acrylonitrile Copolymer samples listed in order from highest average UTS to lowest. [14] (V# means VAIM produced samples)

For other materials, like 50% virgin / 50% recycled polystyrene blend, the strength of VAIM processed parts was enhanced approximately 25% over that of the conventionally molded parts and VAIM produced parts of 75% virgin / 25% recycled polystyrene blend had a maximum strength increase of approximately 22% over conventionally molded samples of the same class of material. [15]

Tensile tests also have been done on samples with different levels of molecular weight. For the samples with same level of molecular weight, the samples with higher level of orientation have the largest increase of percentage in UTS compared to conventional ones. [13]

However, the question as to whether or not VAIM induced molecular orientation levels could influence the degradation behavior of polymeric materials remained unanswered. In this research, biodegradable samples molded by Vibration-Assisted Injection Molding with different levels of molecular orientation and then tested experimentally as they biodegraded. A goal if this is successful would be to monitor and control the degradation rate when VAIM processed biodegradable material were used as implants.

Chapter 3: Vibration Assisted Injection Molding of PLA

3.1 Setting and Parameters

3.1.1 Injection Molding Protocol

The initial parts desired for this research were dogbone specimens. They are simple to make by injection molding and can get the molecular orientation alignments parallel to the mold flow direction easily. Furthermore, it was comfortable to use dog bone shaped parts to have a nice and clear view of molecular orientation under the birefringence lamp. And the samples could be used to perform tensile tests directly with little trimming after production. The polymer material was forced into the mold cavity back and forth alternatively. In this way, the molecular orientation alignments would be created and then locked in the dogbone if the cooling time was short enough. Seen from the picture below, most of the molecular orientation was modified and locked into gage length section of the dogbones. (Figure 3.1)

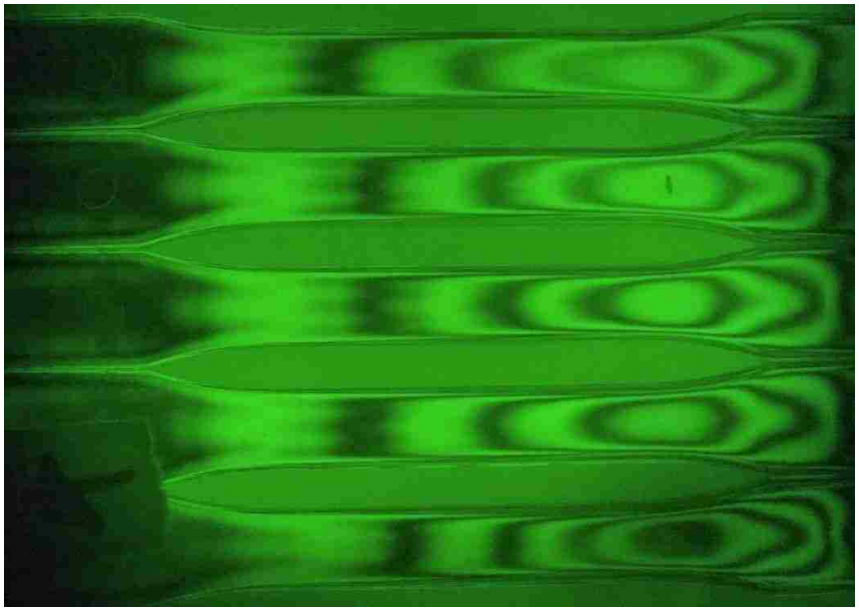

Figure 3.1: Molded samples with locked molecular orientation

The shape and dimensions of the dogbones needed in this research were all determined according to Designation D638-10 of ASTM. (Figure 3.2 and Table 3.1)

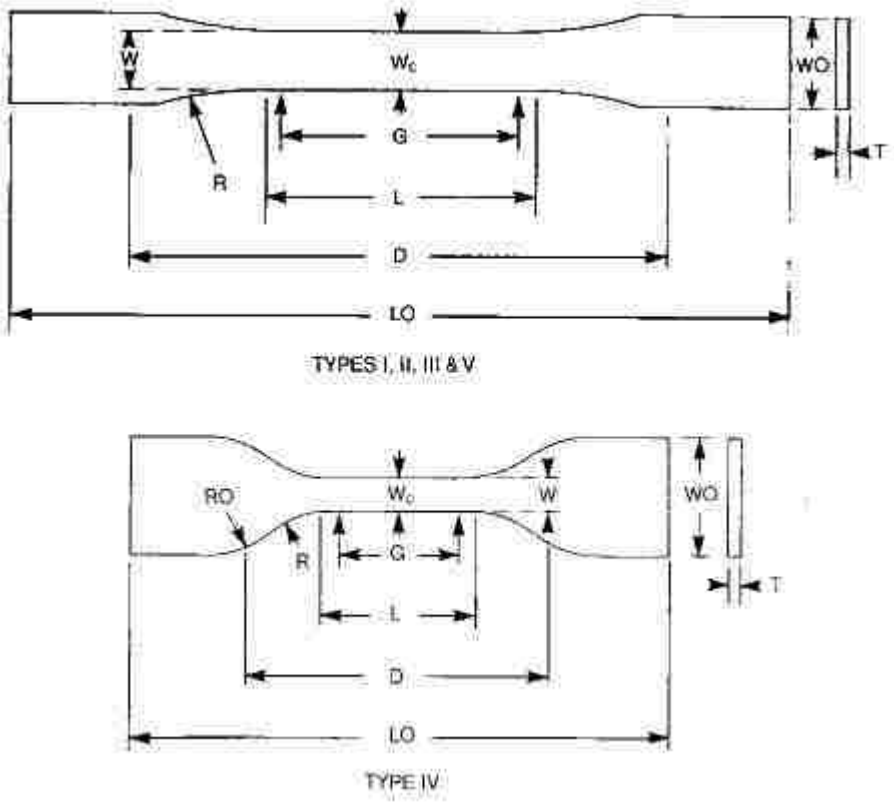

Figure 3.2: ASTM specimen dimensions (D 638) [16]

Dimensions (see drawings)	7 (0.28) or under		Over 7 to 14 (0.28 to 0.55), incl	4 (0.16) or under		Tolerances
	Type I	Type II	Type III	Type IV[B]	Type V[C,D]	
W—Width of narrow section[E,F]	13 (0.50)	6 (0.25)	19 (0.75)	6 (0.25)	3.18 (0.125)	±0.5 (±0.02)[B,C]
L—Length of narrow section	57 (2.25)	57 (2.25)	57 (2.25)	33 (1.30)	9.53 (0.375)	±0.5 (±0.02)[C]
WO—Width overall, min[G]	19 (0.75)	19 (0.75)	29 (1.13)	19 (0.75)	...	+ 6.4 (+ 0.25)
WO—Width overall, min[G]	...	...	...	...	9.53 (0.375)	+ 3.18 (+ 0.125)
LO—Length overall, min[H]	165 (6.5)	183 (7.2)	246 (9.7)	115 (4.5)	63.5 (2.5)	no max (no max)
G—Gage length[I]	50 (2.00)	50 (2.00)	50 (2.00)	...	7.62 (0.300)	±0.25 (±0.010)[C]
G—Gage length[I]	...	...	...	25 (1.00)	...	±0.13 (±0.005)
D—Distance between grips	115 (4.5)	135 (5.3)	115 (4.5)	65 (2.5)[J]	25.4 (1.0)	±5 (±0.2)
R—Radius of fillet	76 (3.00)	76 (3.00)	76 (3.00)	14 (0.56)	12.7 (0.5)	±1 (±0.04)[C]
RO—Outer radius (Type IV)	...	...	...	25 (1.00)	...	±1 (±0.04)

Table 3.1: ASTM specimen dimension data in millimeter (inch) for D 638 [16]

Thickness, T, shall be 3.2 $\pm$ 0.4 mm (0.13 $\pm$ 0.02 in) for all types of molded specimens, and for other Type I and II specimens where possible. [16] D 638 Type I is the designated one for this study.

Before the polymer pellets are placed into the hopper, it is important to dehydrate the material for a certain amount of time until the polymer is dry enough for molding. The reason for doing this is that if the molding material is moist, there could be air bubbles which would be formed by steam and locked in the final products when cooling. Another phenomenon mainly caused by the insufficient drying is silver streaks. Unlike the air bubbles inside the parts, silver steaks are some shining line shaped patterns that appear on the surface of the molded product. This can be considered as an external appearance quality defect. [17] Both the air bubbles and silver streaks can influence the mechanical properties of samples and the testing results. So neither of them should be appear on the final molding products and the specimens with either of these defects cannot be used in the testing.

For the 3051D and 3052D used in this research, the drying instruction were given by the material supplier. Crystalline and amorphous pellets of both 3051D and 3052D look very different. Semi-crystalline pellets are opaque and amorphous pellets are more transparent. [18] (Figure 3.3)

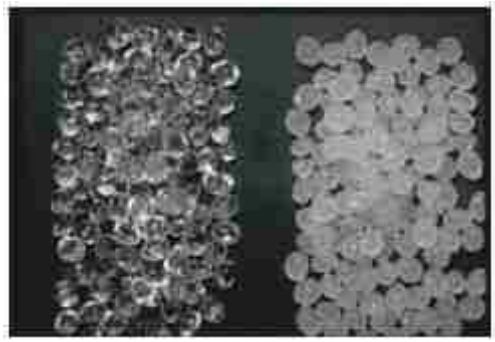

Figure 3.3: Amorphous pellets (left) and semi-crystalline pellets (right) of PLA [18]

According to the process guide provided by NatureWorks, it is recommended that the moisture content should be less than 0.025% (250 ppm) for both amorphous and crystalline materials. The drying curves are shown below in figure 3.4.

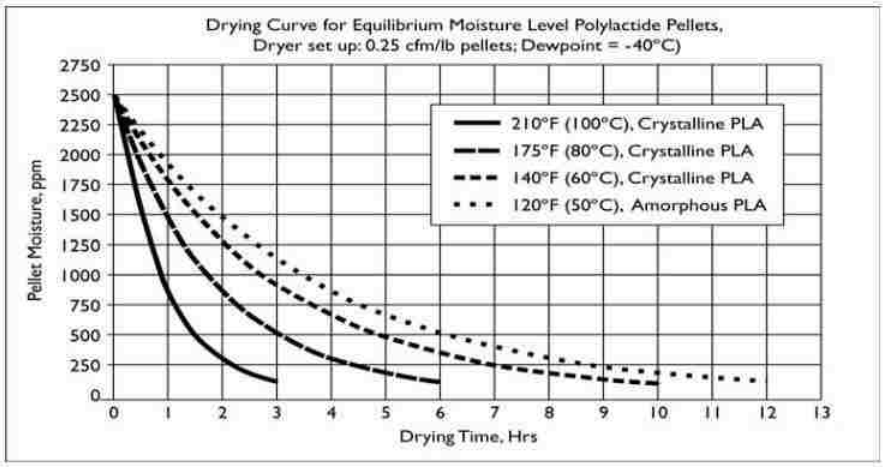

Figure 3.4: Drying curves for amorphous and crystalline polylactide pellets [18]

From Figure 3.4, it is necessary to dry the pellets for at least 7 hours to yield material with a moisture content less than 250 ppm.

After drying, pellets were placed into the hopper which can feed the material into the injecting screw camber. The mold for producing D 638 Type I specimen was made previously by the previous researchers. The exact nominal dimensions of the final products were:

LO = 6.4990 in

WO = 0.7505 in

L = 2.2585 in

W = 0.5040 in

T = 0.1255 in

All the dimensions above meet the required data of D 638 Type I.

3.1.2 Dominant Factors of Injection Molding and VAIM

There are many factors which can affect the molding process and the properties of the final products. Mold cavities and gate size can affect the molding samples directly by determining the shape, dimension, surface quality and even the position of weld line. The runner systems in the mold control directions of the melted material flow. The shear rate difference in the runners and mold could lead to the result of not fully made or not uniformly shaped parts. Injection speed, injection pressure and packing pressure are the parameters which can affect the dogbone quality by causing unexpected changes in dimensions. If the injection speed is too slow, the molten material may be cooled down and frozen before it reaches the end wall of the mold cavity. If the injection pressure or the packing pressure is too low, the final products may have shrinkage along the gage length. However, if either of them is too high, the material would be forced into the gap of the clamped molds causing some flash on the edges of the final parts. In this manner, the clamped molds are pushed away from each other, though for a tiny distance, resulting in the increasing of the sample thickness.

For Vibration-Assisted Injection Molding, other than the factors mentioned above, the vibration frequency and vibration duration are the most dominant factors. By increasing either of them the molecular orientation level can be increased. A common way to quantify the level of molecular orientation imposed on the polymer samples as a result of VAIM is called retardation measurement. [19] (Figure 3.5) High levels of optical retardation are directly proportional to increased levels of molecular orientation.

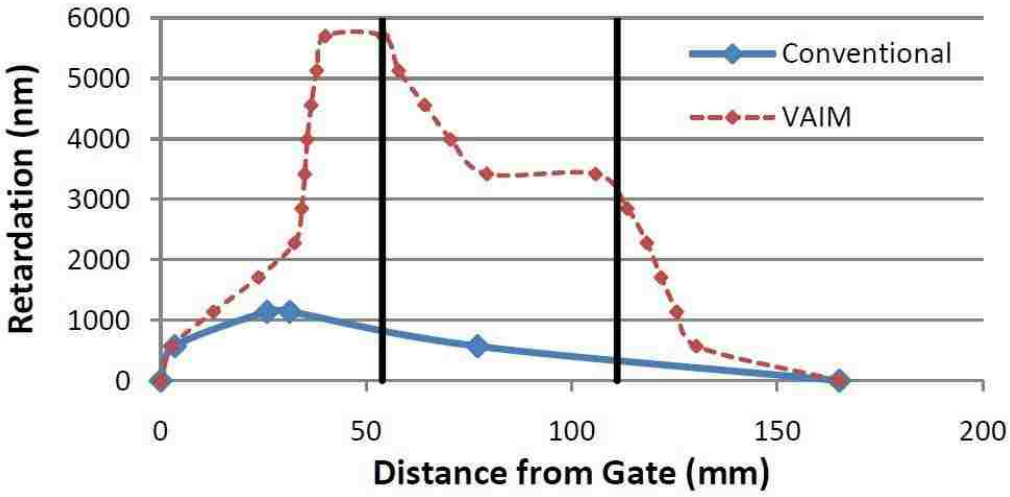

Figure 3.5: Retardation of 3051D PLA of Conventionally and VAIM molded Specimens [19]

It is very clear to see from Figure 3.5 that the sample made by VAIM has a significantly higher level of retardation (and therefore molecular orientation) in comparison to the conventionally molded one. Of course, there are some other factors, like mold temperature, cycling time, cooling time, injection time and injection positions, that can influence the molding results in different ways as well.

3.2 Effects of Process Parameters on PLA Specimens

3.2.1 Parameters Used in Conventional Molding and VAIM

The mold used in this research was designed for D 638 Type I specimens. (Figure 3.6)

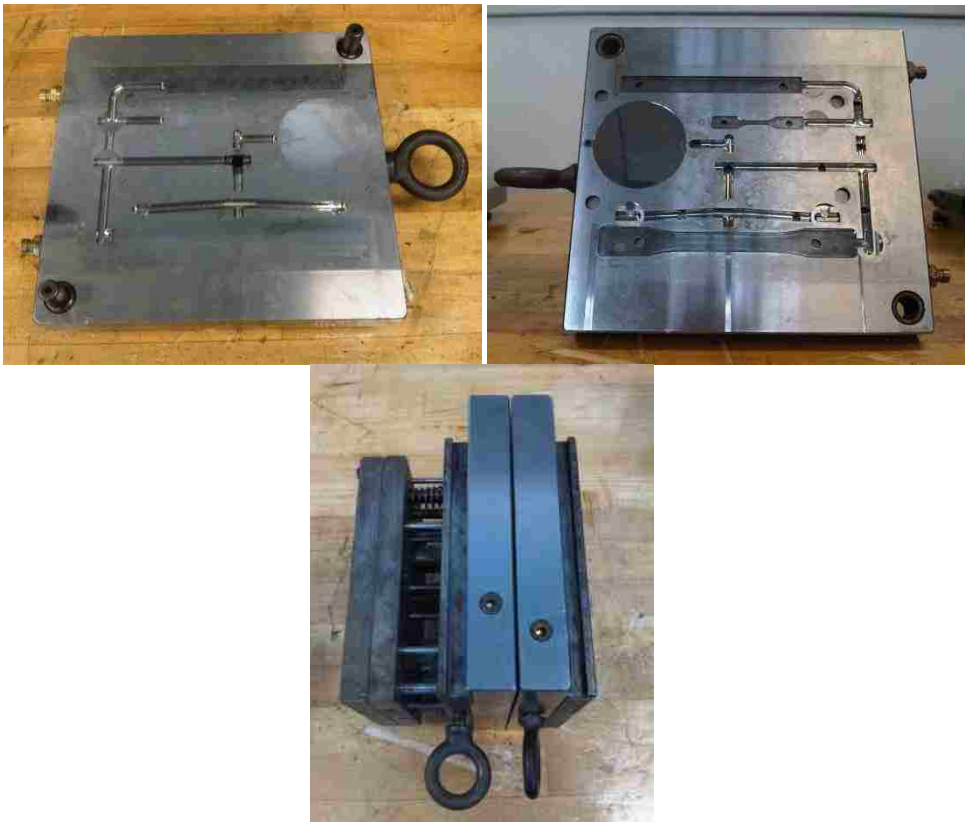

Figure 3.6: Injection molds used in study

Injection time was unified at 20 seconds and cooling time was held constantly at 20 seconds for every molding cycle. Injection speed, injection pressure and packing pressure were set appropriately according to the previous study. (Table 3.2)

Type / Element	Conventional	VAIM_Low	VAIM_Mod	VAIM_High
Injection speed	60%	60%	60%	60%
Injection pressure	20%	30%	30%	50%
Packing pressure	40%	40%	40%	40%

Full injection speed: 71 cm^3 / sec;
Full injection pressure: 1870 kg / cm^2 or 183.26 MPa;
Full packing pressure: 1870 kg / cm^2 or 183.26 MPa;

Table 3.2: Injection speed, injection pressure and packing pressure for each type of samples

Temperatures at different places of the injection unit were recommended based on the Processing Temperature Profile given by NatureWork. (Table 3.3)

Processing Temperature Profile [1]		
Melt Temperature	390°F	200°C
Feed Throat	70°F	20°C
Feed Temperature	330°F	165°C
Compression Section	380°F	195°C
Metering Section	400°F	205°C
Nozzle	400°F	205°C
Mold	75°F	25°C
Screw Speed	100-175 rpm	
Back Pressure	50-100 psi	3.5-6.9 bar
Mold Shrinkage	.004 in/in. +/-.001	

Table 3.3: Molding processing temperature profile [18]

After several test runnings with slightly changes of the temperature combinations, the best temperature file was determined. (Figure 3.7)

Figure 3.7: Final determined temperatures for molding

The four temperatures at the nozzle, front, middle and rear part of the screw were set at 400 F, 380 F, 360 F and 350 F respectively. The conventional samples were made by using all the molding data above. For the parts made by Vibration-Assisted Injection Molding, the primary additional factors were vibration frequency and vibration duration. As it was mentioned before that raising the frequency or the duration can increase the level of molecular orientation, three levels, VAIM_Low, VAIM_Mod and VAIM_High, were classified by applying three groups of vibration data, which were also determined after considerable amount of trials. And for all the molding cycles, there was a delay time of 0 second to begin the vibration. The following figures and data show the VAIM specimens, together with the conventional parts, and their respective vibration parameters.

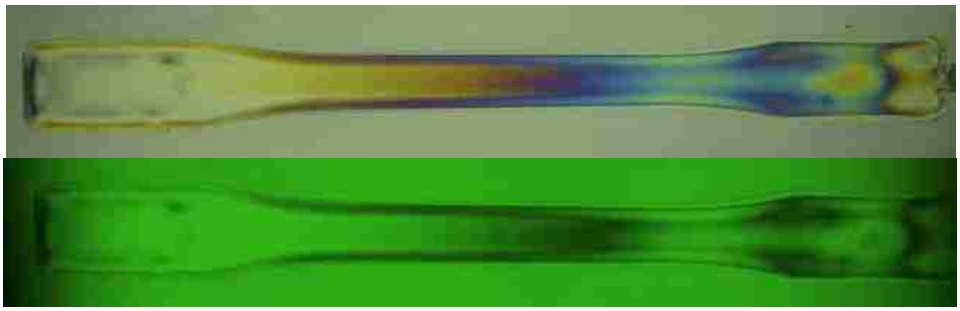

Figure 3.8: Conventional samples

Vibration Duration = 0 sec, Frequency = 0 Hz. (Figure 3.8)

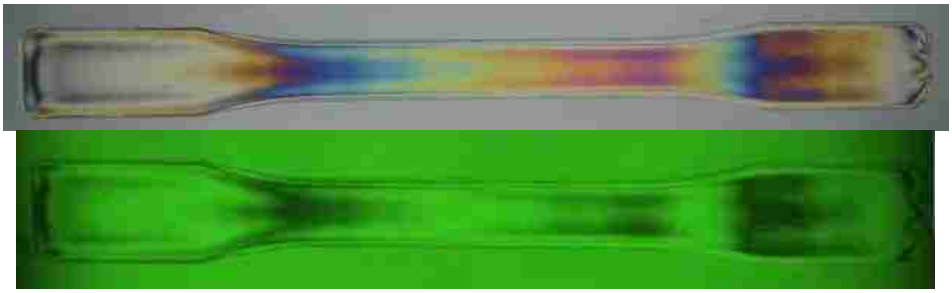

Figure 3.9: VAIM_Low samples

Vibration Duration = 10 sec, Frequency = 4 Hz. (Figure 3.9)

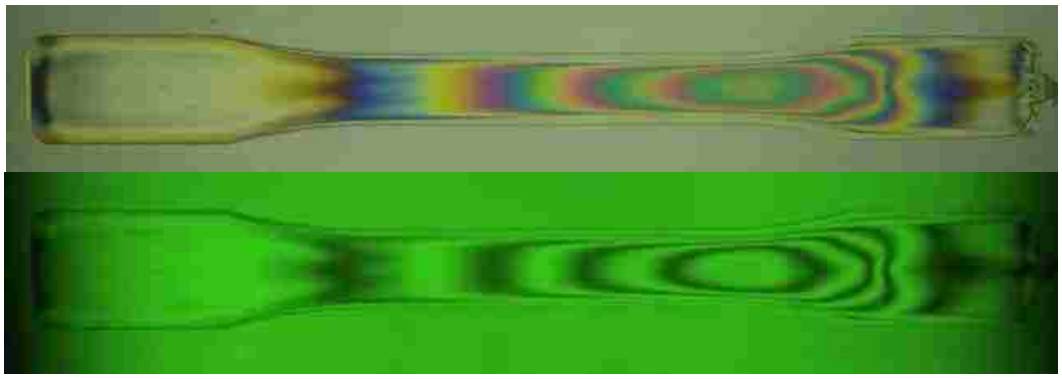

Figure 3.10: VAIM_Moderate samples

Vibration Duration = 15sec, Frequency = 4Hz. (Figure 3.10)

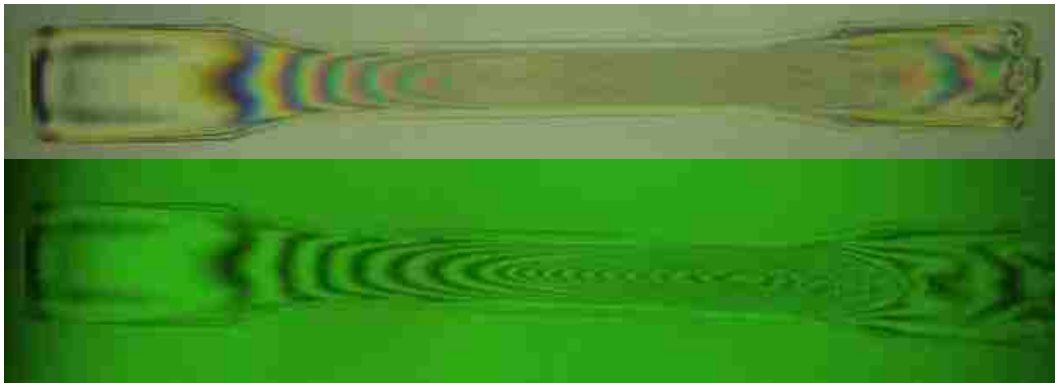

Figure 3.11: VAIM_high samples

Vibration Duration = 15sec, Frequency = 6Hz. (Figure 3.11)

3.2.2 Molecular Orientation and Crystallinity

Molecular orientation and crystallinity share similar ways in influencing the biodegradation process. With an increased molecular orientation level, polymer samples are more resistance against biodegradation, like polymers with a higher percentage of crystallinity. They both have the capability of modifying the orders of molecule alignment, but in different manners. In a crystalline region, a single polymer molecule can form several series of branch like lamellar fibrils, which are full of identical folds along those branches. (Figure 3.12)

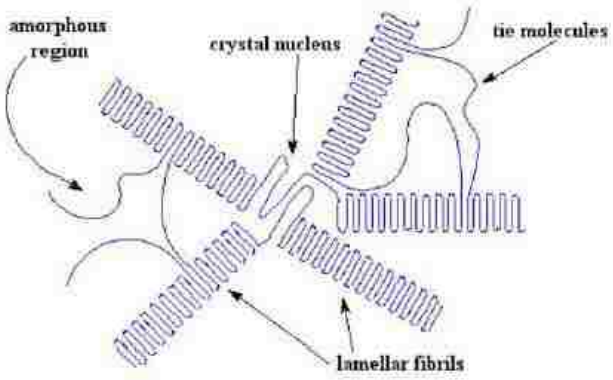

Figure 3.12: Basic element in crystalline region [20]

These fibrils can extend outward from the core molecule into 3-D level, creating a spherulite section. [19]

Molecular orientation can affect both amorphous and crystalline regions. Amorphous regions are between the crystalline regions. They can be aligned in certain directions, which means aligned more in order. Figure 3.13 gives a clear schematic of crystalline region before and after alignment.

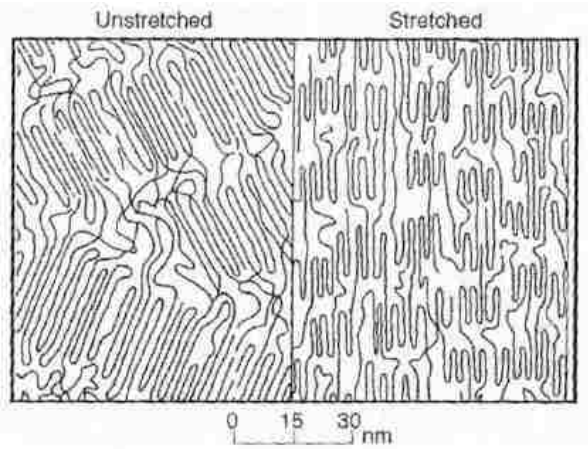

Figure 3.13: Crystalline region before (left) and after (right) alignment [21]

3.2.3 Secondary Processing after Molding

After injection molding, there were still secondary processes that needed to be done. Once the parts were molded successfully, the samples were kept in a

refrigerator until all the later molded parts were done. In this way, the variation of initial biodegradation condition of all the dogbones was reduced to be as small as possible.

The specimens molded for tensile tests were kept intact as the original dogbone shape. For the parts used for other kind of tests, they were sent to be cut into rectangular bars from the gage length area. A Powermatic band saw (Figure 3.14) was used to do the cutting work and Figure 3.15 shows how the rectangular parts were cut from dogbones.

Figure 3.14: Powermatic band saw

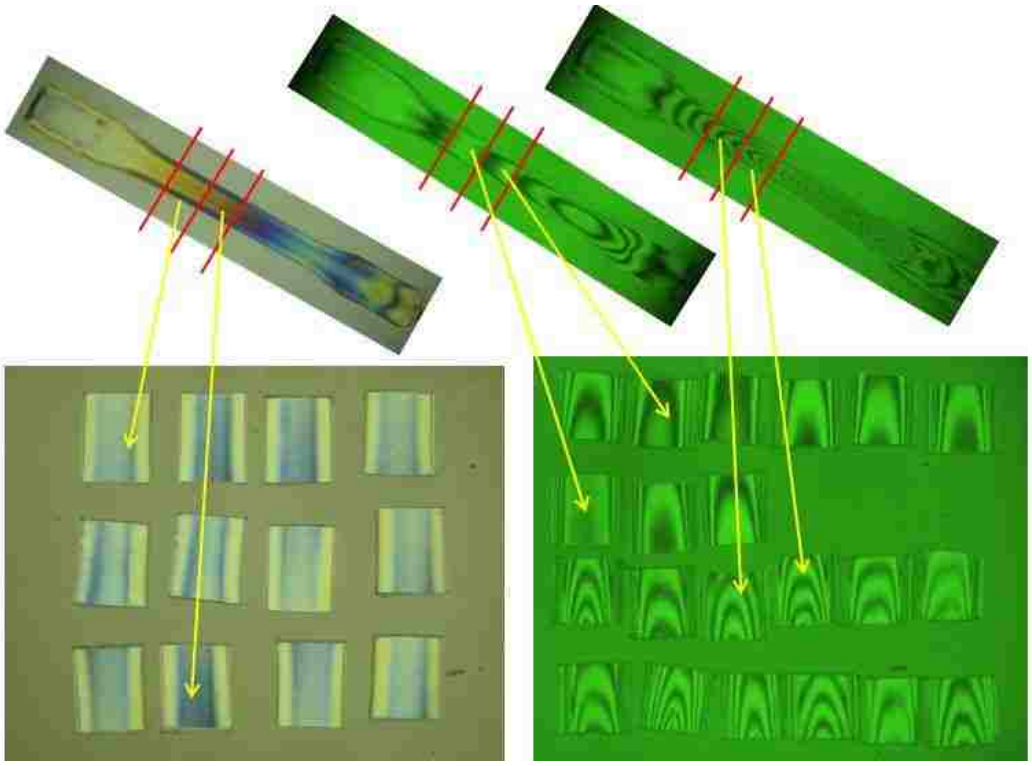

Figure 3.15: Rectangular parts cut from dogbones

The size of the resulting rectangular samples was suitable for the multi-well plates used for incubation storage during biodegradation. From Figure 3.15, it is easy to see that the machining does not change the molecular orientation levels within the samples at all. They were still easy to be classified according to the levels of molecular orientation.

Some trimming of the samples was necessary after cutting. Because rough edges can be formed by sawing and the heat generated from friction could cause remelting and refreezing along the cutting edge. The way used in this study to get rid of the rough edges was just simply sanding the edges off with sand paper manually, which didn't change the molecular orientation either.

All of the specimens were marked individually in order to trace and compare them during and after tests if necessary. (Figure 3.16 and Figure 3.17)

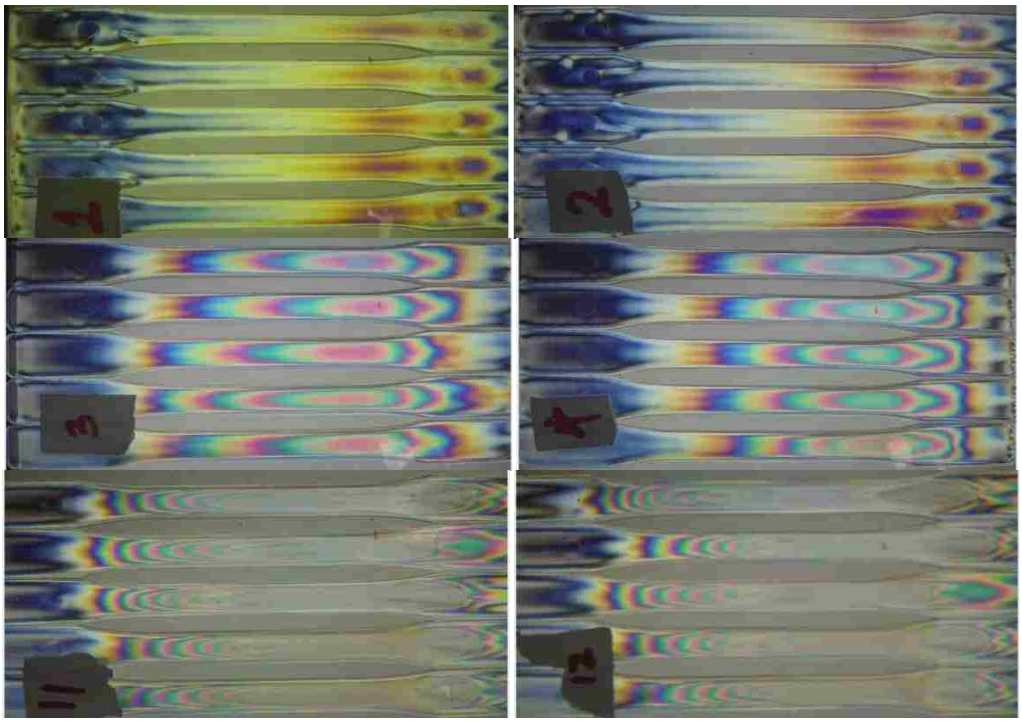

Figure 3.16: Some of the marked dogbones

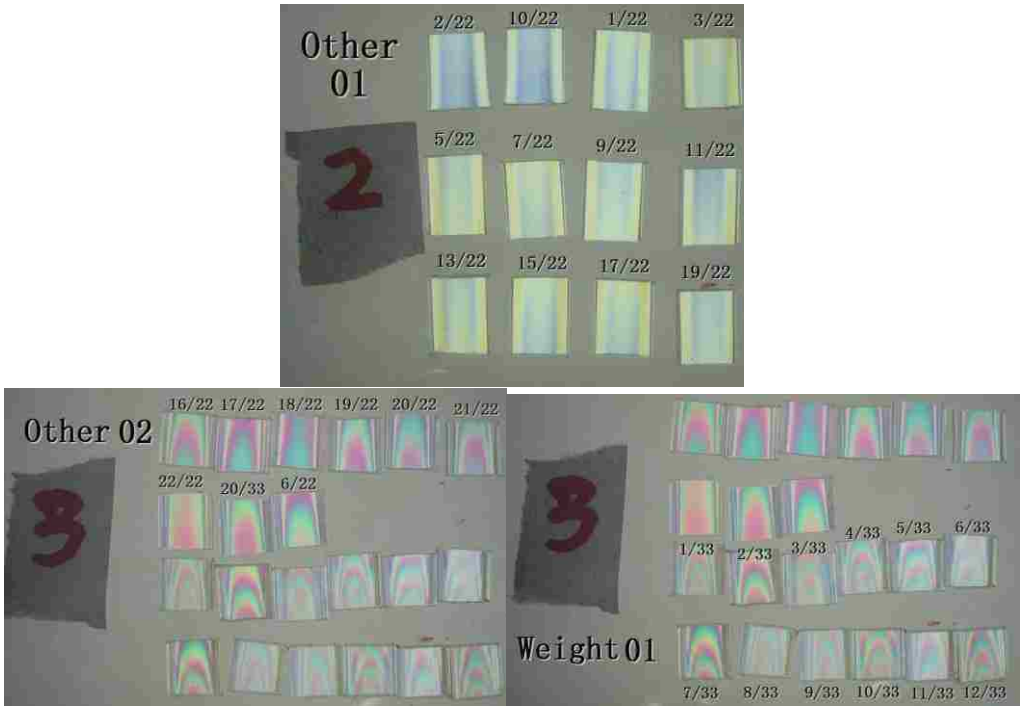

Figure 3.17: Some of the marked rectangular parts

After applying VAIM, all PLA samples were ready to be taken into the biodegradation lab to do the sterilization and then be incubated for the tests, which will be discussed in Chapter 4.

Chapter 4: Biodegradation Tests

4.1 Description and Preparation for Tests

4.1.1 Test Schedule

PLA biodegradation is a relatively long time progress. It could take months to get fully degraded. So it was planned as a 21 week long research for the nonenzymatic degradation and 60 days for the enzymatic degradation at the very beginning.

For weight measurement in every testing time, three rectangular samples would be measured for nonenzymatic degradation and another three rectangular samples for enzymatic degradation. The initial weights of all the rectangular samples for this test were recorded before incubation. In tensile test, four dogbones were tested in nonenzymatic degradation and three dogbones in enzymatic degradation. Mean while, two rectangular specimens for nonenzymatic degradation and three for enzymatic degradation were prepared for DSC, TGA and GPC tests as a little amount of material was needed to do each of these four tests. FT-IR testing was also applied, but only two of the nonenzymatic incubated samples were experimented with in testing weeks.

Basically speaking, all the tests for nonenzymatic degradation were performed every two weeks during the first few weeks until week 12. Because no significant degradation behaviors were detected in all the applied tests except GPC test, it was decided to perform all tests every four or six weeks in order to extend the entire testing time and get better or significant biodegradation data. For enzymatic degradation, all tests were applied every ten days.

Considering the fact that the molecular orientations in the conventionally molded samples and the VAIM_Low samples were similar, and the biodegradation behaviors of these two types of parts were not so different according to the previous studies, VAIM_Mod samples were treated as VAIM_Low in this research, abandoning the original VAIM_Low specimens. So conventional, VAIM_Low and VAIM_High became the only kinds of samples used in this research and tested according to the same schedule.

From all of the above, the number of samples needed was determined as shown in the following table. (Table 4.1)

Tests (N.E.+E.) / Sample type	Weight Measurement	Tensile Test	DSC + TGA + GPC + FT-IR
Conventional	33+21	64+21	22+21
VAIM_Low	33+21	64+21	22+21
VAIM_High	33+21	64+21	22+21

Table 4.1: Sample amount needed in research (N.E.=nonenzymatic, E.=enzymatic)

4.1.2 Biodegradation Solution

To simulate the fluid environment inside our human body, Phosphate Buffered Saline, which is one of the mostly used buffered solutions in vitro, and Tris-HCl Buffer, for enzymatic biodegradation, were used in this research. The concentration of PBS for nonenzymatic biodegradation is listed below in Table 4.2.

Concentration / Salt	In mmol / L	In g / L
NaCl	137	8.00
KCl	2.7	0.20
$Na_2HPO_4 \cdot 2H_2O$	10	1.44
KH_2PO_4	1.76	0.24

Table 4.2: Concentration of different salts in PBS

10X PBS was made and then it was diluted to 1X. The following is the protocol of how to make the 10X PBS of 1 liter:

I. Starting with 800 ml of distilled water;

II. Adding 80 g of NaCl;

III. Adding 2 g of KCl;

IV. Adding 14.4 g of Na_2HPO_4 ;

V. Adding 2.4 g of KH_2PO_4 ;

VI. Adjusting the pH value to 7.4 with HCl;

VII. Adding distilled water to 1 L of total volume.

2 L of 10X PBS was made for this study and it was sterilized at $120^{O}C$ for 15 minutes previously. After the sterilization, 200 ml of PBS was taken out and made into 2 L of 1X PBS as the initial solution for the samples and more 1X PBS can be made later in the research if necessary. The rest of the 10X PBS was stored in a refrigerator for further use.

For the enzymatic biodegradation, 10X Tris-HCl (0.5M Tris Base, pH7.6) was prepared:

Trizma Base: 61 g;

Distilled water: 1000 ml;

It was adjusted to a pH of 7.6 using concentrated HCl and then stored at room temperature. Diluting 1:10 with distilled water before use and adjusting pH if necessary.

4.1.3 Enzyme Factors During Biodegradation

Enzymes were added into the biodegradation environment of polymers in some previous researches. Some researchers investigated that enzymes, such as proteinase K, bromelain and pronase, were able to accelerate the rate of PLA degradation. And among those enzymes, proteinase K was the most effective one for PLA biodegradation. [22]

Proteinase K is able to digest native keratin and the dominant cleavage catalyzed by prteinase K is the peptide bond which is adjacent to the carboxyl group. Hydrolytic and enzymatic degradation of PLA/PEO/PLA triblock copolymers were studied and it was proved that the presence of proteinase K strongly accelerated the biodegradation speed of the hydrogels as the PLA domains were attacked and penetrated by this enzyme. [23] 0.8 mg of proteinase K was filled into 3 ml of 0.05 M pH=8.6 Tris buffer for every immersing gel disks. Figure 4.1 shows that for enzymatic degradation of hydrogel, a weight loss of 56.9% was observed compared with the weight loss of 5% for the pure hydrolytic degradation after 80 hours of storage. [24]

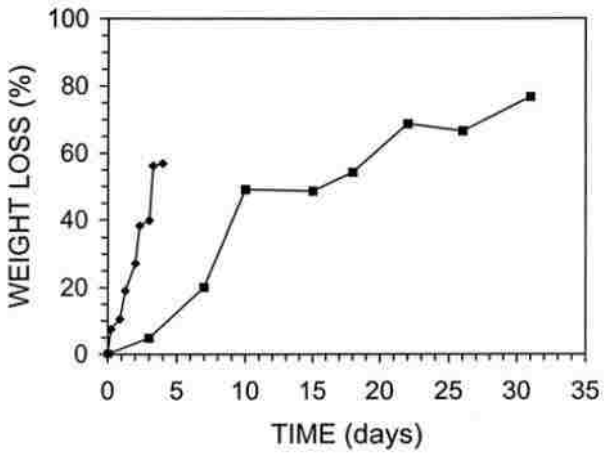

Figure 4.1: Comparison of weight loss of hydrolytic and enzymatic degradation of $PLA_{264}/PEO_{182}/PLA_{264}$ [24]

The concentration of proteinase K used in this study was 2 mg in 1X of Tris-HCl.

4.1.4 Storage and Incubation

As all the samples were labeled, the dogbones and the rectangular bars were kept in the storage containers and the multi-well plates in order. (Figure 4.2 and Figure 4.3)

Figure 4.2: The container for dogbone storage

Figure 4.3: The multi-well plates for rectangular sample storage

Before all the samples were put into their containers and plates, they needed to be sterilized. All specimens were put into the ethanol with a concentration of 80% and kept for about 30 minutes. Then the specimens were submerged into the pure ethanol for about 10 minutes. After this, all specimens were washed with 1X PBS to get rid of the ethanol residue and moved into the containers, which were sterilized in the same way.

All samples were completely submerged into PBS and incubated at 37 ^{O}C constantly. As the solution could get dry and vaporized, in order to keep the solution level always above the samples, it was necessary to check and refill the solution over time.

For the tested samples, it's better to keep them for later checking and redo of some experiments. So all the used parts were grouped, marked and stored in refrigerator.

4.2 Tests Applied over PLA Biodegradation

There are many ways to monitor the degree of biodegradation. The basic idea is to understand it from microcosmic and macroscopic points of view. So GPC, FT-IR, DSC, TGA, weight measurement and tensile test were applied to investigate the molecular, chemical, thermal and mechanical properties of testing materials during degradation.

4.2.1 GPC

GPC is known as Gel Permeation Chromatography. It is used to measure the molecular weight of soluble materials. From previous studies, there are three main activities that occurr during biodegradation. Decreasing of molecular weight happens first, then followed by a reduced tensile strength and even later by the mass reduction as Figure 4.4 shows below. Measuring the molecular weight was one of the most important tests performed to study polymer biodegradation as the decreasing of molecular weight presents first and could be found in a relatively short time.

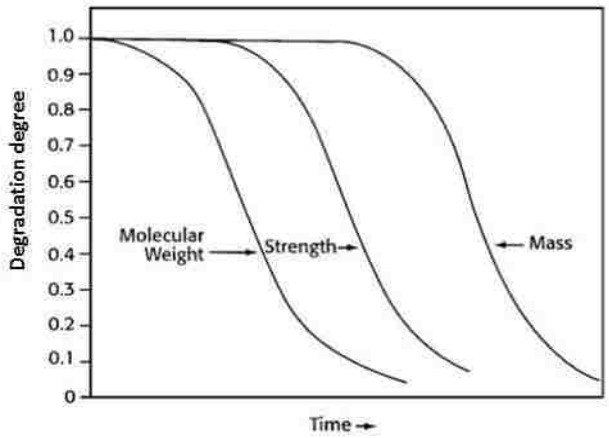

Figure 4.4: Polymer biodegradation activities over time [25]

A GPC test mainly involves separation of molecules with different molecular weights. Dissolved material is injected into the analyzing equipment and flows through columns full of porous beads. The analytes with lower molecular weight can travel into or kept inside the pores more easily than the analytes with high molecular weight. In this way, it takes more time for the low molecular weight particles to get through all the columns, increasing their retention time. The basic and rough understanding of how to determine the molecular weight is that materials with standard molecular weights (Figure 4.5) were tested previously and their retention times were recorded correlatively, then after injecting the test sample into the system, the retention time was measured and compared to the standard times, and the software in computer was able to calculate the molecular weight based on the standard weights and the compared retention times given by the test.

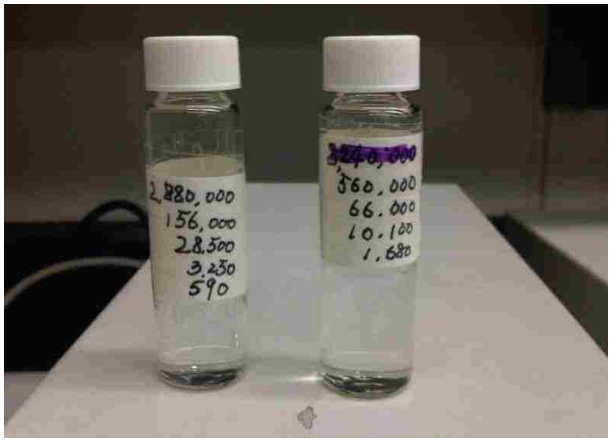

Figure 4.5: Solutions with standard materials dissolved

There are several ways of defining and measuring the molecular weight. Two common ways of doing that are using number average molecular weight, Mn, and weight average molecular weight, Mw. The calculations of the two are shown below:

$$\bar{M}_n = \frac{\sum_i N_i M_i}{\sum_i N_i}$$

$$\bar{M}_w = \frac{\sum_i N_i M_i^2}{\sum_i N_i M_i}$$

One problem of using Mn is that as not each polymer molecule has a long chain-like structure, some untypical molecules have very short chain-like structure. If the untypical molecules were measured together with the typical ones, the short molecules will affect the result significantly by reducing the average molecular weight. To reduce this influence, it is better to us Mw as the molecular weight contribution is considered.

Initial molecular weights of all kinds of specimens were measured before incubation. The solvent for dissolving PLA parts was THF (Tetrahydrofuran). The GPC analyzing system was composed of an operating monitor, a flow pump, an inject/load switch, column tunnels, a differential refractometer and a personal computer which provided the testing results. (Figure 4.6)

Figure 4.6: GPC testing system

The software used to analyze the GPC data was PL Caliber®, version 7.03, ©1992-1998 Polymer Laboratories, which gave the values of Mn and Mw automatically.

4.2.2 FT-IR

FT-IR is short for Fourier Transform Infrared. Fourier Transform Infrared spectroscopy is an experiment that probes the interaction of infrared light with chemical bonds in molecules. When the infrared radiation hits some matter, it can be absorbed, causing some chemical bonds to vibrate. [26]

Light is formed by two kinds of waves, one is an electric wave and the other is a magnetic wave. These two waves travel in two separate planes which are perpendicular to each other. The third plane, which is perpendicular to the two planes mentioned above, is the light traveling plane. The electric part of light can interact with molecules. [26] This electric vector of light has a sine wave manner and the amplitude is changing over time. The wavelength is the distance between two adjacent wave peaks, valleys or same points in phase. (Figure 4.7)

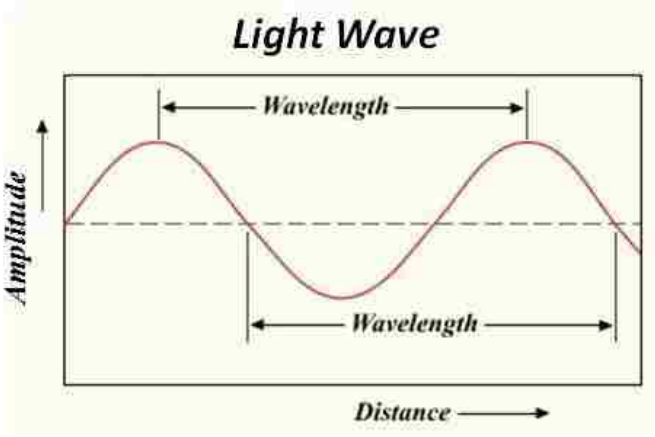

Figure 4.7: Light in sine wave and wavelength

λ is being used to represent wavelength, while W is representing wavenumber. The two elements have a relationship as shown below:

$$W = \frac{1}{\lambda}$$

λ is measured in cm, so W is in unit of cm^{-1}. Wavenumber is the most common way of denoting the different kinds of light. The wavenumber of a particular light wave is proportional to the energy contained in the light wave. The Energy-Wavenumber equation is:

$$E = hcW$$

where:

E = Light energy;

c = The speed of light ($3x10^{8}$ meters/second);

h = Planck's constant ($6.63x10^{-34}$ Joule-second);

W = Wavenumber; [23]

So there is more energy in the light with higher wavenumber. In this study, the infrared lights are defined between 650 cm^{-1} to 4000 cm^{-1}.

All matter in the universe gives off infrared radiation above absolute zero. [26] When infrared radiation meets the molecules in matter, it can be absorbed and cause the chemical bonds to vibrate. Light with a certain wavenumber can be absorbed by the only correlated chemical bond or bonds, no matter what the rest of the molecule structures are. In this way, measuring the absorption or the transmittance of the light with different wavenumbers can determine the types of chemical bonds or the function groups included in molecules and the rough

amount of them. If there are more of one kind of bond, the percentage of the absorption or the transmittance of this correlated wavenumber would be more.

In this research, PLA is degraded during hydrolysis, generating more hydroxyl end groups and carboxyl end groups as shown in Figures 2.5 and 2.6. For polymers, the carboxyl bond and the ester bond are more constrained when they are in position of the end of the molecules, compared with they are being the pendent backbone groups along the polymer chain. [19] Then the absorption or the transmittance peak corresponding to the wavenumber of the bond correlated light should shift a little bit to a higher number, indicating that the bonds in the end groups need more energy to get vibrated.

As explained above, C-O, C=O and O-H are the general bonds which should be detected and in which the shifting peaks might be found. The equipment used in this research was a PerkinElmer® Spectrum 100 FT-IR spectrometer. (Figure 4.8)

Figure 4.8: PerkinElmer® Spectrum 100 FT-IR spectrometer

4.2.3 DSC

Differential Scanning Calorimetry (DSC) is a well-known technology which is applied in many thermal research areas. Characteristic caloric values, such as heat capacity, heat of transition, kinetic data, purity and glass transition, can be obtained with this measurement. [27]

2910 Modulated DSC equipment was used in this research. (Figure 4.9) This was a heat flux DSC with a disk-type measuring system.

Figure 4.9: DSC 2910 MDSC equipment from *Du Pont Instruments*™

There were two measuring spots inside the heating chamber, which is adiabatic from the outside environment. One was used to locate the testing sample and the other one was for a reference sample. (Figure 4.10) The sample was kept in a small sealed aluminum pan and the reference sample was just a sealed aluminum pan without any object inside. (Figure 4.11)

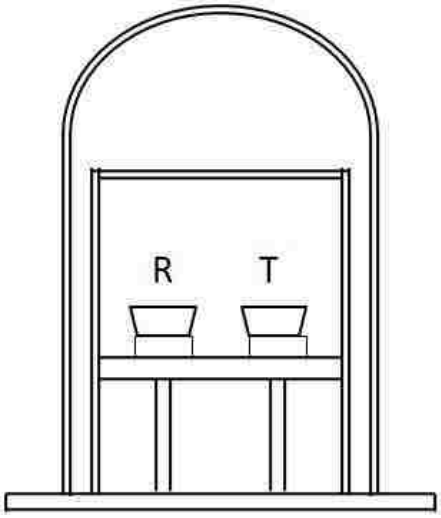

Figure 4.10: DSC heating chamber with reference sample (R) and testing sample (T)

Figure 4.11: Aluminum pan (right) and its aluminum cover (left)

The two samples were seated on the two spots symmetrically in order to achieve equally high heat flow flowing through the pans. If the two samples were ideally symmetrical (same pans and same testing materials inside the pans), the heat flow rates traveling into and out from the two pans would be the same and the differential temperature signal ΔT (originally a difference of electric potentials measured and captured by system) could be zero. [27] So the balance could be disturbed by adding testing material into one of the pans and in this way, a differential signal of temperature or electric potential would be generated.

The DSC test in this study was used to look for the glass transition temperature, Tg, and the changes of it during biodegradation. Similarly as melting temperature, which is denoted as Tm and depends on the molecular weight of the polymer, Tg decreases due to the reduction in molecular weight. [28] During degradation, long molecule chains break into shorter ones resulting in the reduced molecular weight.

Glass transition is a step change of the heat capacity on heating or cooling. [27] (Figure 4.12) The Tg range of polymeric glass is from -100^{o}C to 300^{o}C, whereas for silicate or inorganic glass, it ranges from 500^{o}C to 1000^{o}C. So polymers are more suitable for DSC measurement. [27]

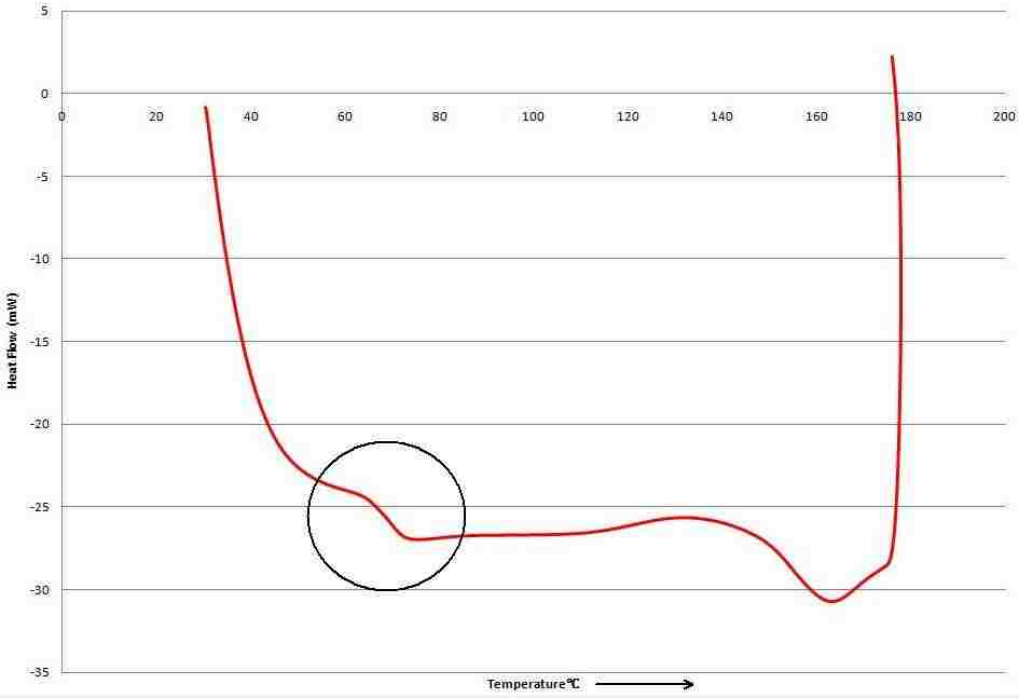

Figure 4.12: Experimental DSC curve with glass transition process circled

The heating or cooling rate was critical for DSC test. For samples with the mass between 10 mg – 20 mg, if the cooling or heating rate is over 20 K/min, the glass transition temperature error would be 3 K to 20 K. So the recommended

cooling rate for testing 10 mg – 20 mg samples is between 10 K/min and 20 K/min, or $\geqslant$5 K/min. Also the maximum temperature should be at least 15 K to 30 K above Tg and the minimum temperature should be 50 K below Tg. [27]

In this research, PLA specimens with weight between 10 mg- 20 mg were cut from the rectangular parts. The initial heating temperature or equilibrium temperature was 30^{o}C and the samples were heated to 180^{o}C with the heating rate of 5^{o}C/min or 5 K/min for avoiding large errors. The software, Universal Analysis for Windows 95/98/NT version 2.6D (©1998-1999 TA Instrument, Inc), was used to gain the glass transition temperature, Tg.

4.2.4 TGA

Thermogravimetric Analysis (TGA) is a technology which can be used to measure a material's thermo stability. The changes in mass of a substance can be detected and graphically recorded when cooling or heating, as a function of temperature or time. And the curve or trace provided in TGA is known as a thermogram or thermo-weighing curve. [29]

Thermal degradation begins with the breaking of the bonds which form the weakest links in polymer molecule chains. As there are irregularities that can act as the weak links, most polymers decompose at a substantially lower temperature than the comparable smaller molecules. [30] In this way, the onset temperature of thermal degradation would be shifting to a slightly higher value over biodegradation time. So the shifting value or the shifting rate may be the

characteristic factors which indicate the biodegradation rates of different specimens.

In this study, a sample with a weight between 10 mg and 20 mg thermal degraded in a heated nitrogen environment when the temperature rises from 30^{o} C to 600^{o} C, with the heating rate of 10^{o} C/min, inside of the heating tunnel of this TGA Q500 testing equipment showed in Figure 4.13. And Universal Analysis 2000, version 4.7A (©1998-2009 TA Instruments-Waters LLC) was utilized to do data analysis.

Figure 4.13: TGA Q500

4.2.5 Weight Measurement

Weight measurement is the most common test applied in biodegradation research. It gives the most intuitive and obvious data of degradation results. All weighing samples in this study were weighed and recorded before incubation. For the specimens stored with enzyme, they were simply wiped with Kimwipes®, same as some researchers did in some previous studies, to get rid of the moisture which would influence the measuring results. However for the samples incubated without enzyme, another dry way of measuring the weight was performed. After the samples were taken out from the incubator, they were dried in an oven, LINDBERG / BLUE M® D-5226-Q oven (Figure 4.14), for about 2 hours before taking the measurement.

Figure 4.14: LINDBERG / BLUE M® D-5226-Q oven

4.2.6 Tensile Testing

For mechanical property study of polymeric materials, elastic modulus, ultimate tensile strength and elongation at break are the typical properties that need to be investigated. Within the biodegradation of polymers, all the values of these properties were supposed to be higher for the specimens with stronger ability of resist degradation. Based on this, it was theorized that an increased level of molecular orientation should yield a higher mechanical strength parallel to the molecular orientation direction. [19]

ASTM D 638 Type I was the standard research sample molded and tested in experiment. And an INSTRON 5667 C 9620_30 kN Tensile Testing Machine (Figure 4.15), which was connected to a computer for appropriate data obtaining and analyzing, was used. The software installed in the connected computer to translate and analyze the tensile data was Bluehill 2 (Instron Bluehill Software© 2005, Version 2.13). This software could provide the strain-stress curve and data over testing time. So it was very convenience to have the tensile test results with it.

Figure 4.15: INSTRON 5667 C 9620_30 kN Tensile Testing Machine (left) and zoomed in view of a dogbone held in the pliers (right)

According to ASTM D638-2010 standard, the speed of testing was set at 5 in/min for all tensile testing dogbones. (Table 4.3)

Classification	Specimen Type	Speed of Testing, mm/min (in./min)	Nominal Strain[C] Rate at Start of Test, mm/mm· min (in./in.·min)
Rigid and Semirigid	I, II, III rods and tubes	5 (0.2) ± 25 %	0.1
		50 (2) ± 10 %	1
		500 (20) ± 10 %	10
	IV	5 (0.2) ± 25 %	0.15
		50 (2) ± 10 %	1.5
		500 (20) ± 10 %	15
	V	1 (0.05) ± 25 %	0.1
		10 (0.5) ± 25 %	1
		100 (5)± 25 %	10
Nonrigid	III	50 (2) ± 10 %	1
		500 (20) ± 10 %	10
	IV	50 (2) ± 10 %	1.5
		500 (20) ± 10 %	15

Table 4.3: Designations for tensile test speed of each standard type [16]

However, elastic modulus was not measured well enough to provide any valuable data or result and the elongations seemed to be so randomly distributed. So the ultimate tensile strength was the main research target property in this research.

With all the experiments mentioned above, the biodegradation manner of the PLA samples should be well monitored and sufficient results or conclusions would be given.

Chapter 5: Results and Discussion

During 39 weeks of nonenzymatic biodegradation and 54 days of enzymatic biodegradation, all the six tests, Gel Permeation Chromatography (GPC), Fourier Transform Infrared (FT-IR), Differential Scanning Calorimetry (DSC), Thermogravimetric Analysis (TGA), weight measurement and tensile testing was performed.

5.1 GPC Test Results and Discussion

The GPC test was used to determine the molecular weight. As Chapter 4 mentioned, the decreasing of PLA molecular weight should be detected during biodegradation processes. The results that were produced follow.

5.1.1 Nonenzymatic Biodegradation Test

In GPC testing, 10% of changes were considered significant due to the precision of the testing system. Figure 5.1 shows the decreasing of normalized molecular weight for conventionally molded, VAIM_Low molded and VAIM_High molded samples over the biodegradation duration.

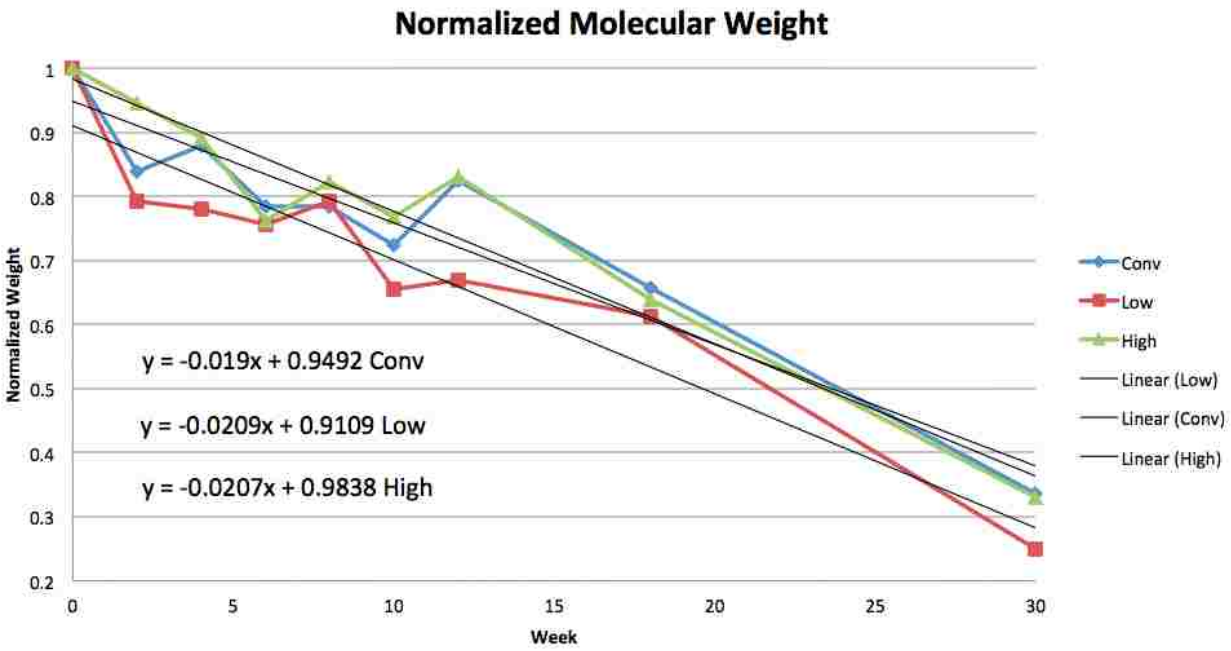

Figure 5.1: Decreasing of molecular weight for all types of samples during incubation for nonenzymatic biodegradation

It is clear to see that after two weeks of incubation, conventionally molded samples and VAIM_Low molded samples each had an over 10% change of decreased molecular weight. For the VAIM_High molded parts, the 10% of difference in molecular weight did not show up until 4 weeks of incubation. During the 30 weeks of degradation, the normalized molecular weight of VAIM_High samples was always higher than that of the VAIM_Low samples. After 30 weeks, the normalized molecular weight of VAIM_Low specimens decreased to about 0.25 of the initial value, while the conventional and VAIM_High parts had about 0.33 of their initial weights.

Linear trendlines for the three kinds of samples are also included in Figure 5.1. Judging from the slope of the three resultant equations, VAIM_Low specimens seemed to degrade slightly faster than VAIM_High ones as -0.0209 for VAIM_Low and -0.0207 for VAIM_High. Table 5.1 also gives the normalized

molecular weights at selected weeks, indicating that VAIM_Low samples degraded faster than VAIM_High ones. But the degradation rate of the conventional specimens was not the slowest over all periods of time during degradation. This result was not expected.

Incubation Time (Week)	Normalized Molecular Weight		
	Conventional	VAIM_Low	VAIM_High
0	1	1	1
2	0.8389	0.7938	0.9462
8	0.7852	0.7938	0.8231
18	0.6577	0.6125	0.6385
30	0.3355	0.2500	0.3308

Table 5.1: Normalized molecular weights in week 0, 2, 8, 18 and 30 for nonenzymatic biodegradation

5.1.2 Enzymatic Biodegradation Test

After 10 days of biodegradation, the VAIM_Low parts showed a significance of 10% change in molecular weight, followed by the VAIM_High parts on Day 23. The conventional parts showed no significance until Day 33, at which time, VAIM_High and VAIM_Low parts both increased in molecular weight. (Figure 5.2 and Table 5.2)

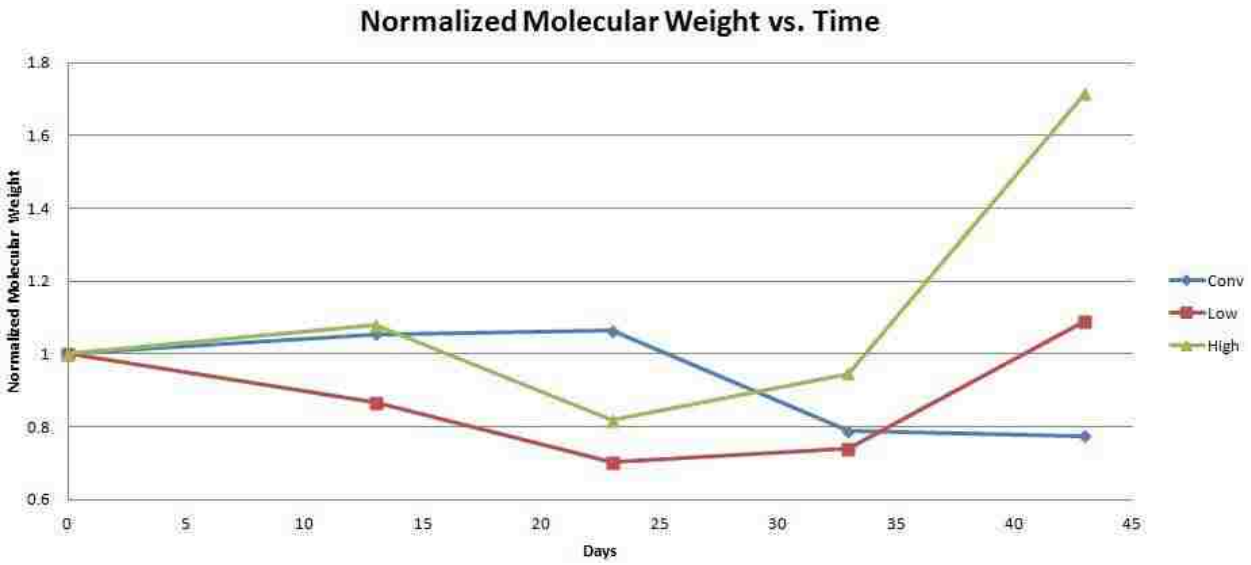

Figure 5.2: Normalized molecular weights vs. incubation time for enzymatic biodegradation

Incubation Time (Day)	Normalized Molecular Weight		
	Conventional	Low_VAIM	High_VAIM
0	1	1	1
13	1.0544	0.8674	1.0792
23	1.0640	0.7026	0.8181
33	0.7885	0.7396	0.9468
43	0.7747	1.0906	1.7158

Table 5.2: Normalized molecular weights on day 0, 13, 23, 33 and 43 for enzymatic biodegradation

The unexpected growth of molecular weight may be due to the bonded proteinase K with the polymer molecules at the ends. As it was known at the beginning of this study that the weight average molecular weight of PLA is about 100 000 Da (Da=Dalton=g/mol). The molecular weight of proteinase K is about 28 900 Da. So if the enzymes stick on the sides of polymer molecules during degradation and are still there during GPC tests, the investigated molecular weight could increase, even the original polymer molecules had degraded or been scissored to some degree. In this way, the increased molecular weight may be contributed by both of the polymer and the enzyme.

5.2 FT-IR Test Results and Discussion

As some of the chemical bonds could be broken and some more chemical bonds could be generated in hydrolysis, all these symptoms can be found in FT-IR testing curves indirectly. In this study, the growing and shifting of peaks were supposed to show the generation of chemical bonds and the bond characters depending on the status or the position along the polymer chain for nonenzymatic biodegradation specimens.

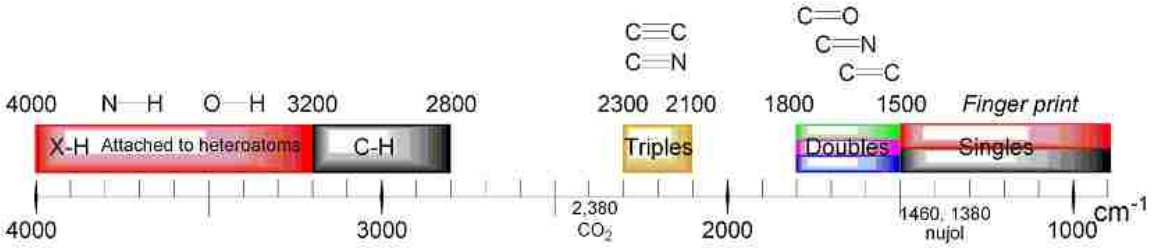

Figure 5.3: List of some chemical bonds and their corresponding wavenumbers in cm^{-1} [31]

Every chemical bond has its correlated absorption of wavenumber. As Figure 5.3 shows, each kind of chemical bond corresponds to a range of the wavenumber values. In lactic acid chain, the oxygen-hydrogen bond, O-H, absorbs infrared light at wavenumbers between 3100 cm^{-1} and 3600 cm^{-1}. The carbon-oxygen single bond, C-O, absorbs from 1150 cm^{-1} to 1400 cm^{-1} approximately. And for the carbon-oxygen double bond, C=O, the absorption of infrared light is between 1600 cm^{-1} and 1800 cm^{-1}.

Figures 5.4~5.7 give the infrared light transmittance (in percentage) of O-H bond correlated wavenumbers over the incubation time, indicating how much of the infrared light was transmitted. So the absorption is the subtraction of the transmittance from 100%. In this case, the absorption peak and the transmittance

peak should be at the same spot. For the nonenzymatic biodegradation, the peak values of transmittance at the very beginning of this research (Week 0) were all around 98.7%. (Figure 5.4) In week 6, the transmittance peak of the conventional samples was about 98.5%, while the other two were around 98.8%. (Figure 5.5) When the study went to week 18 (Figure 5.6), the conventional sample peak reached under 96.5%, however the other two peaks were still not lower than 98.7%. In Week 32, the peak values of conventional, VAIM_Low and VAIM_High were around 95.4%, 96.5% and 97.5% respectively. (Figure 5.7)

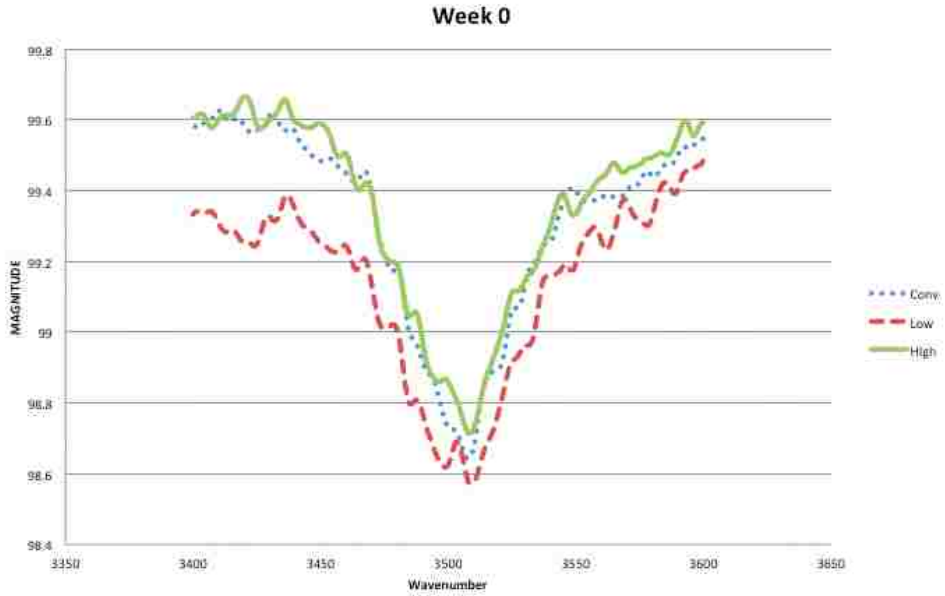

Figure 5.4: Transmittance of the infrared light corresponding to O-H bond in week 0

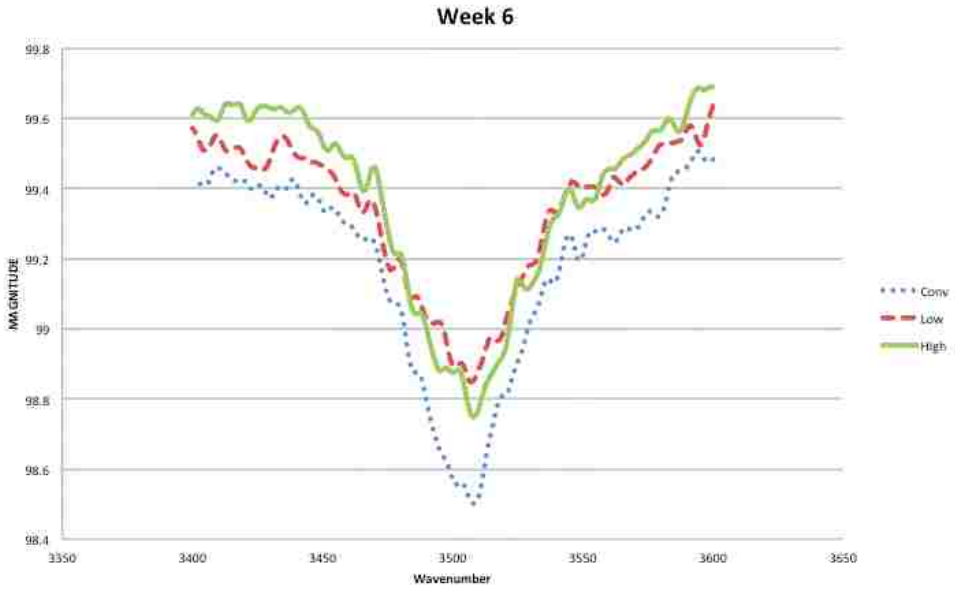

Figure 5.5: Transmittance of the infrared light corresponding to O-H bond in week 6

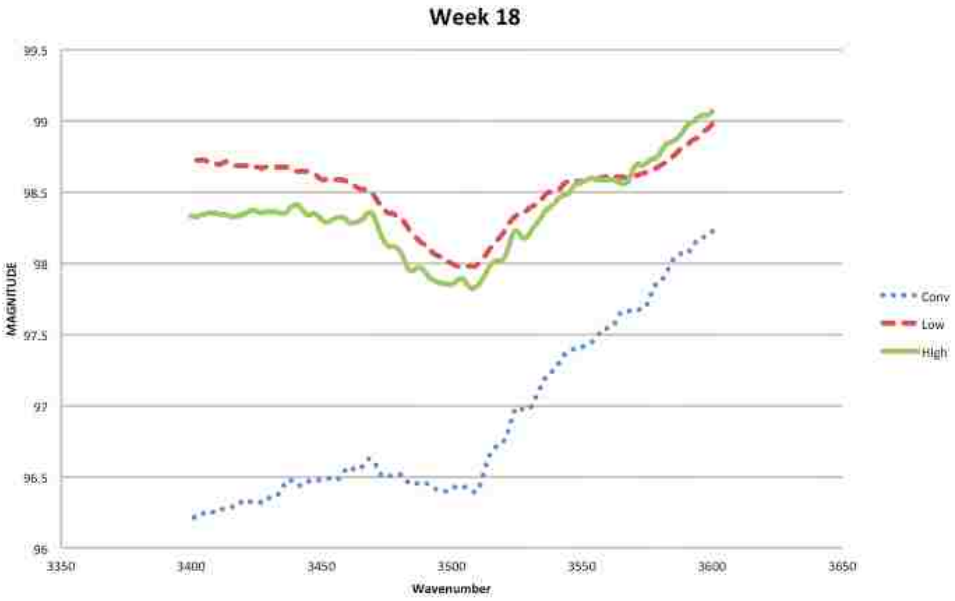

Figure 5.6: Transmittance of the infrared light corresponding to O-H bond in week 18

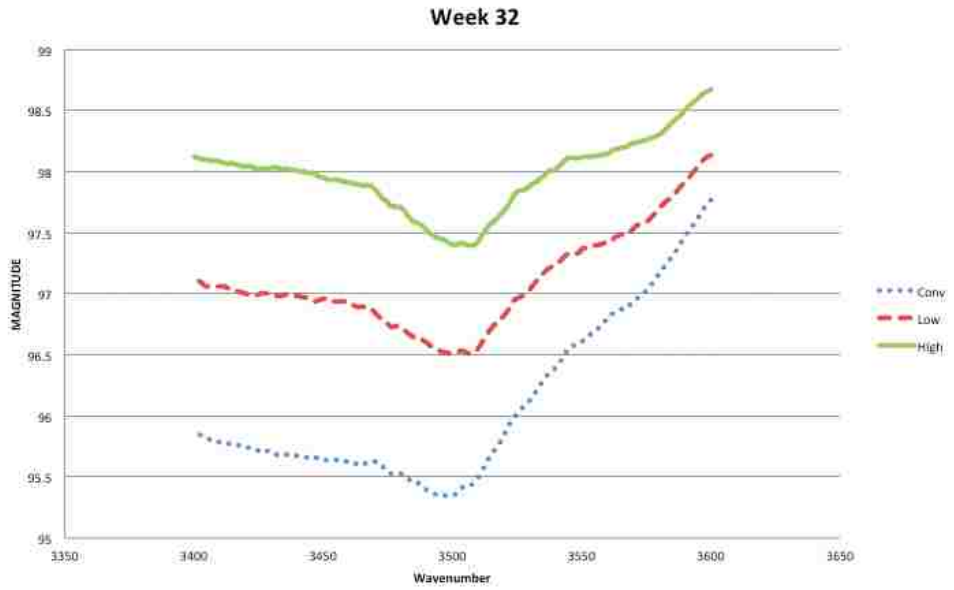

Figure 5.7: Transmittance of the infrared light corresponding to O-H bond in week 32

For the investigation of carboxyl and carbonyl groups, though the shifting peaks were supposed to be discovered over incubation time, it seemed that neither the C-O peak nor the C=O peak were shifting at all. Additionally, the C-O and C=O peaks in the weeks other than Week 0 seemed to be randomly higher or lower than the peaks in Week 0, which was unusual and hard to explain. (Attachment I and Attachment II)

From all of the above, it can be concluded that the conventionally molded samples were generating more hydroxyl groups or at a faster speed, indicating that the polymeric chains in conventional samples were easier cleaved by the water molecules during hydrolysis in comparison with the VAIM_Low and VAIM_High specimens. This increase in hydroxyl bonds represented the increase in degradation.

5.3 DSC Test Results and Discussion

Chapter 4 has already explained that the reduction of molecular weight may cause a decrease of the glass transition temperature, Tg. This phenomenon should be found in experimentation.

5.3.1 Nonenzymatic Biodegradation Test

The plots presented in Figure 5.8 show the changes of glass transition temperature over time. Conventional samples had the highest initial Tg, about 61.6°C. For VAIM_Low and VAIM_High samples, initial values of the corresponding Tgs were 60.1°C and 60.6°C. Though decreasing as a whole, the Tg of conventional samples was always higher than the other two until Week 30. And Tg of VAIM_Low was higher than Tg of VAIM_High most of the time until Week 30. After Week 30, Tgs of VAIM_Low and VAIM_High were higher than Tg of conventional specimens.

The trendlines and their equations verify that the Tg of VAIM_High samples decreased the slowest and that of conventional samples decreased the fastest, as the slops of VAIM_High, VAIM_Low and conventional are -0.115, -0.1268 and -0.2112 respectively. (Figure 5.8)

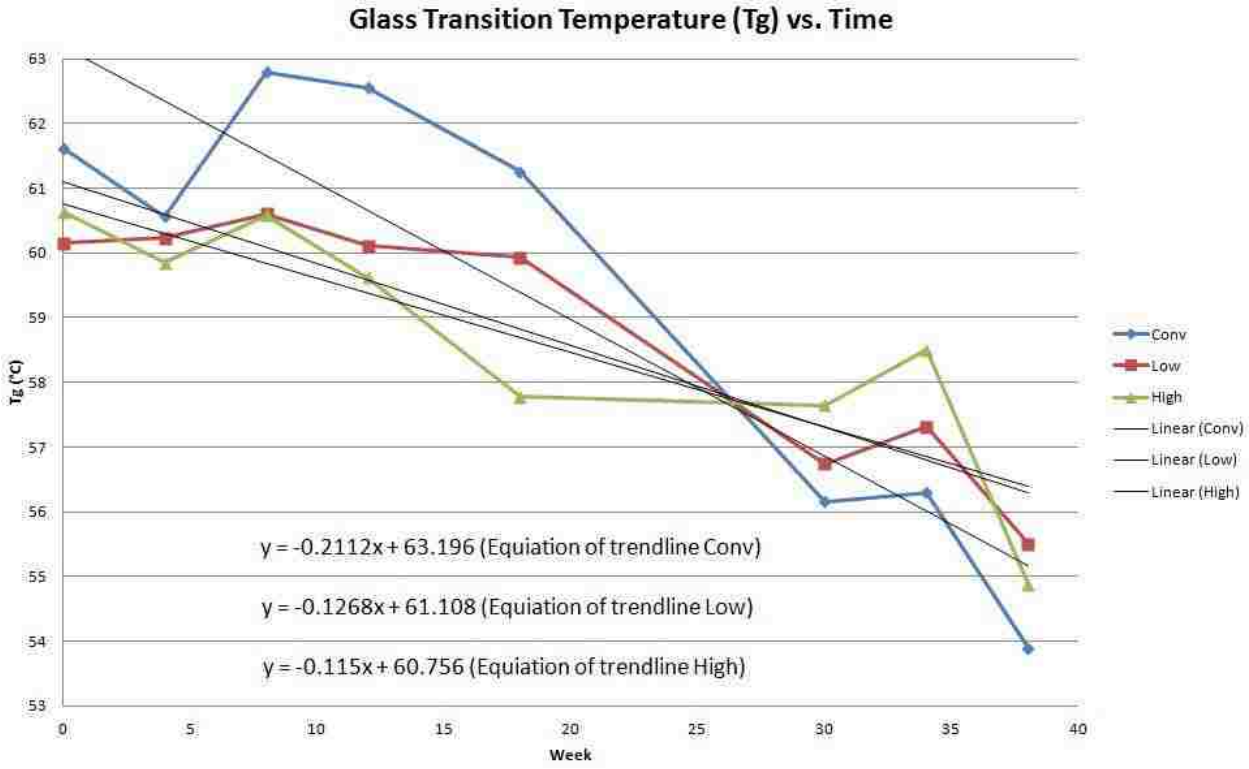

Figure 5.8: Glass transition temperature vs. incubation time for nonenzymatic biodegradation

All degrading samples exhibited an increase in their Tgs after Week 6. This may be the result of the absorbance of water molecules.

Vibration-Assisted Injection Molding could arrange the molecular orientation level and also may break the long chain molecules into slightly shorter ones. As the decreasing of Tg due to the reduction of molecular weight, VAIM led to VAIM samples to have smaller molecules and conventional parts to have larger molecules. (Table 5.3) In this way, the Tg of conventional samples was higher in the beginning weeks. But conventional specimens degraded faster, so its Tg was decreasing faster and was below Tgs of VAIM_Low and VAIM_High samples eventually.

Sample Type	Conventional	Low_VAIM	High_VAIM
Initial M. W.	107154	95554	62477

Table 5.3: Initial molecular weight values of conventional, VAIM_Low and VAIM_High parts

5.3.2 Enzymatic Biodegradation Test

All of the plastics tended to stay along distinct paths, with the VAIM_High having the highest Tg except on Day 33. (Figure 5.9) The VAIM_High parts had the strongest intermolecular forces, perhaps due to the better alignment of molecules, more dipole and Van Der Waals forces as the dominant factors in this case.

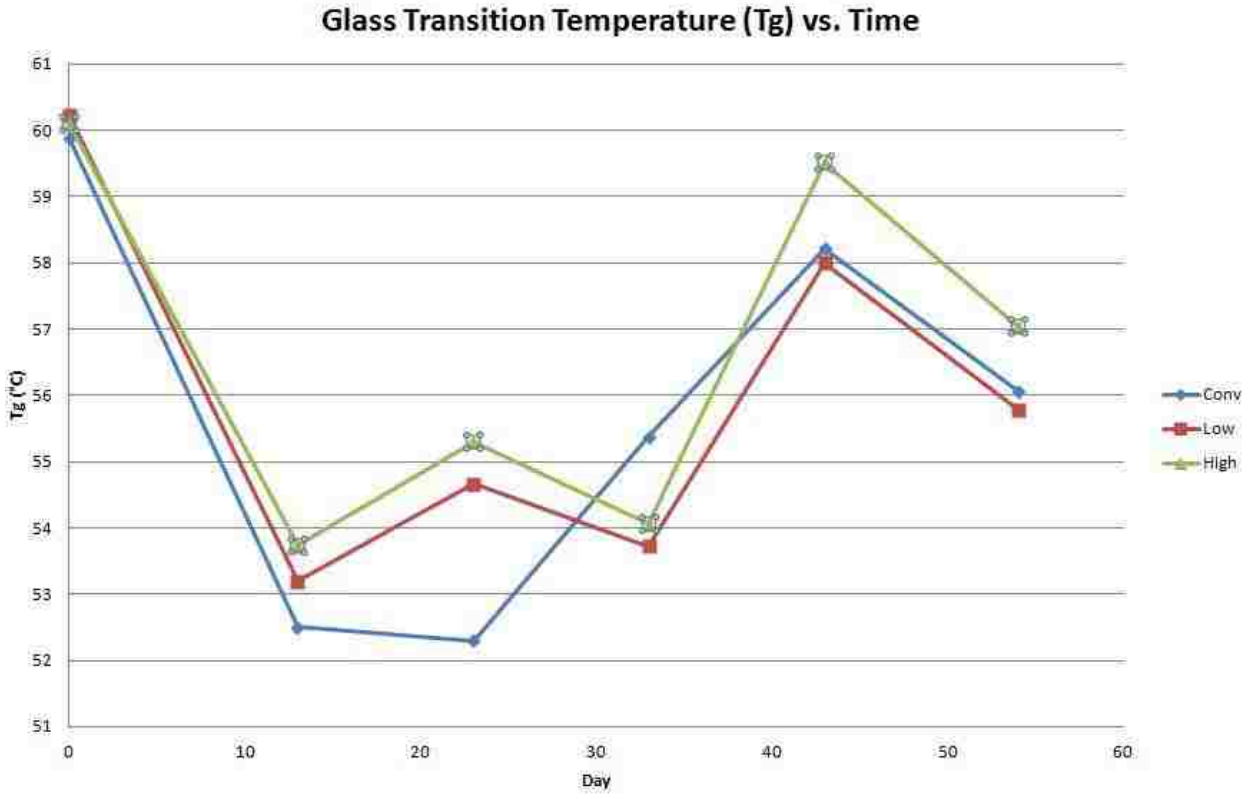

Figure 5.9: Glass transition temperature vs. incubation time for enzymatic biodegradation

Figure 5.9 also shows that the increasing of Tgs happened after about 23 days, which was ahead of that for nonenzymatic incubation (6 weeks). This indicated that the proteinase K might catalyze the biodegradation process.

5.4 TGA Test Results and Discussion

In this section, as mentioned in Chapter 4 that materials with smaller molecules started the thermal degradation at a slightly higher temperature, the experimental target was to explore the onset temperature of thermal degradation shifting towards higher temperature zone to prove that the VAIM manufactured samples could degrade slower than the conventional ones by comparing their onset temperatures.

5.4.1 Nonenzymatic Biodegradation Test

The onset temperature in a TGA test is the temperature at which samples begin to lose weight. It denotes how free or how easily the material gets evaporated or thermal degraded.

In Figure 5.10, plots of onset temperatures of different samples throughout the degradation process express that all onset temperatures decreased eventually instead of increasing. In the first few weeks, the onset temperature of VAIM_Low samples increased ahead of the onset temperatures of conventional and VAIM_High were increased and the significant increasing of onset temperatures of conventional and VAIM_High samples was seen from Week 4.

The reduction of onset temperature in this study, contrary to the assumption mentioned in Chapter 4, could be the result of that before degradation, for large molecule polymers, the intermolecular forces and bonds are the dominant restriction, which need more energy to break, compared with the Van Der Waals force, the dominant restriction for smaller molecule polymers after degradation, it is easier to break. Thus, the evaporation or thermal degradation would be carried out with less energy for polymers after certain degrees of degradation and this could lead to the decreasing of the onset temperature.

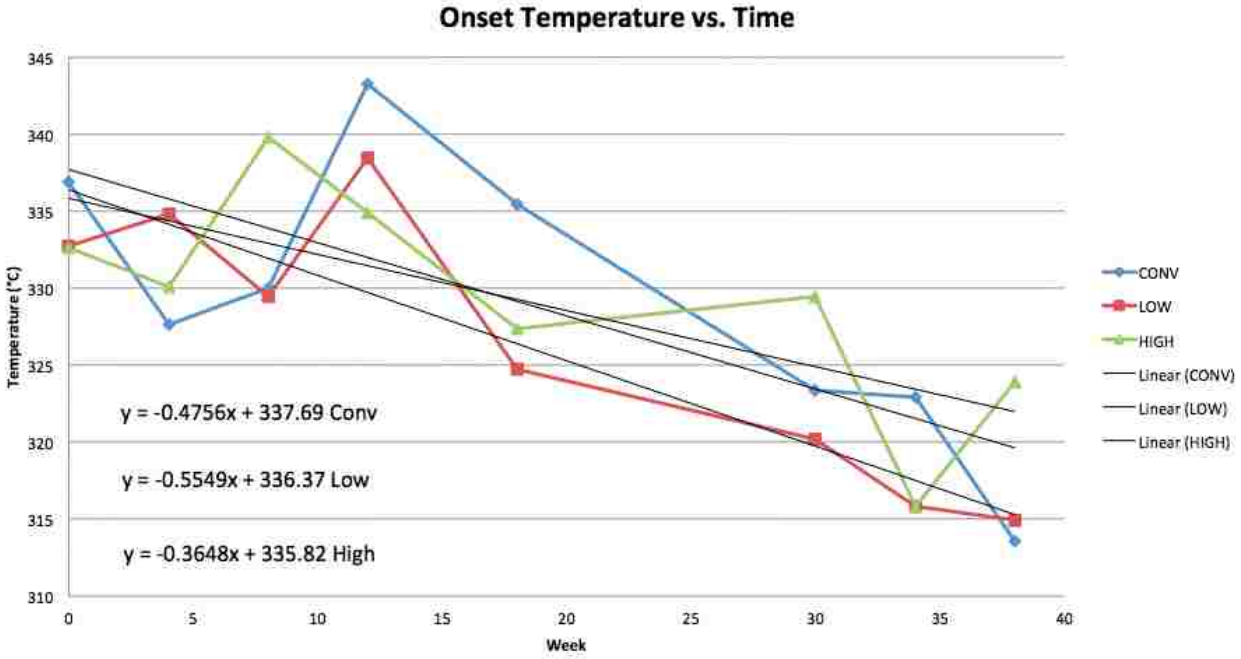

Figure 5.10: Onset temperature vs. incubation time for nonenzymatic biodegradation

Equations of the linear trendlines are provided in Figure 5.10 as well. VAIM_High specimens had the least absolute value of slope, meaning that its decreasing rate of onset temperature was the slowest.

5.4.2 Enzymatic Biodegradation Test

The onset temperatures of VAIM_Low and VAIM_High samples were increasing in the first few days of degradation, while the increasing onset temperature of conventional parts was not being discovered until Day 13. (Figure 5.11) In comparison with four weeks for the nonenzymatic biodegradation, the increasing of onset temperatures of conventional and VAIM_High samples presented within two weeks, which meant a faster degradation process with the effect of enzyme.

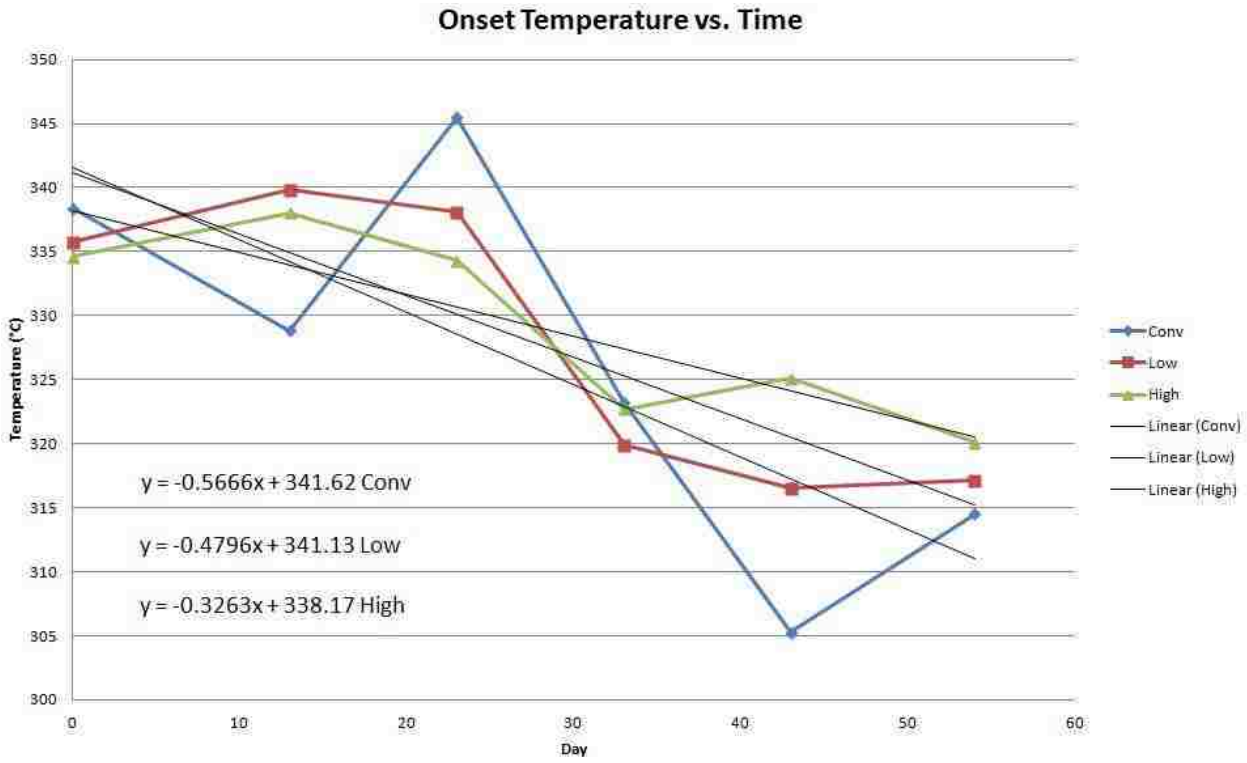

Figure 5.11: Onset temperature vs. incubation time for enzymatic biodegradation

The slopes illustrated that VAIM_High samples had the slowest decreasing rate of the onset temperature, while the conventional samples had the

fastest. This may also conclude that VAIM samples could degrade relatively slower.

5.5 Weight Measurement Results and Discussion

Although the decreasing of weight happens after the decreasing of molecular weight and tensile strength, it really could take a considerably long time to discover the change in weight. In this research, the weight measurement was still carried out in order to seek the variation of it.

In Figure 5.12 and Figure 5.13, the masses of the three types of samples are displayed with respect of incubation time.

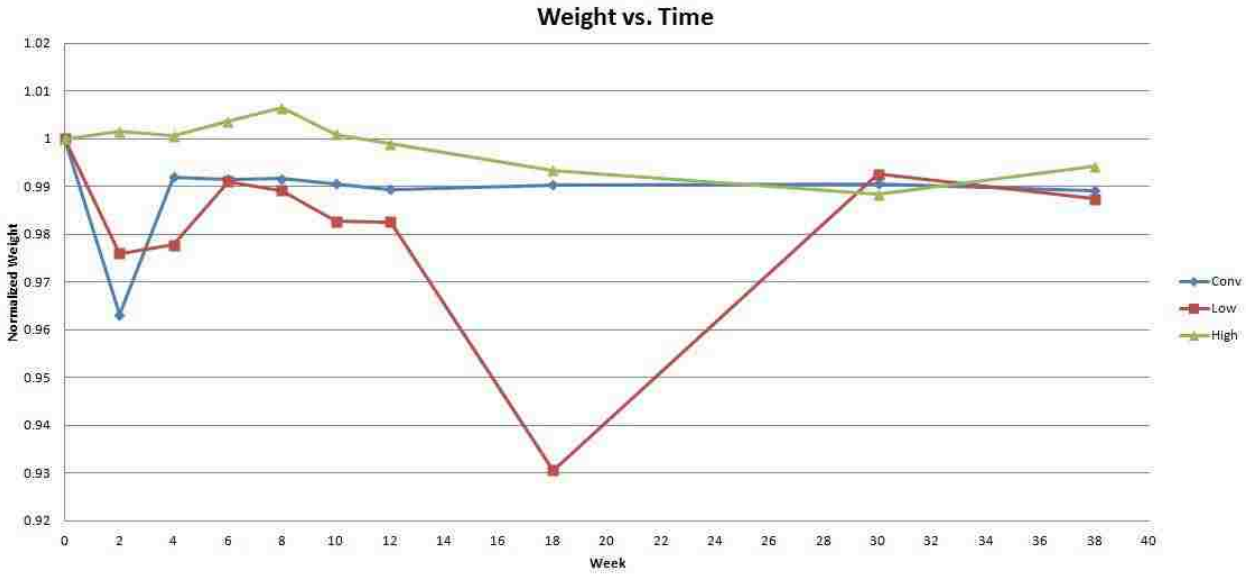

Figure 5.12: Mass vs. incubation time for nonenzymatic biodegradation

For the immediate drop in weight of nonenzymatic biodegradation, it may result from the erosion of the outer surface followed by a sample swelling. [20] This only happened to the conventional and VAIM_Low specimens, and the drop degree of conventional was higher than that of the VAIM_Low.

The conventionally molded specimens for enzymatic incubation increased in mass after Day 13 may due to the absorbance of the enzymatic buffer. And no signal of any preliminary drop was found. (Figure 5.13)

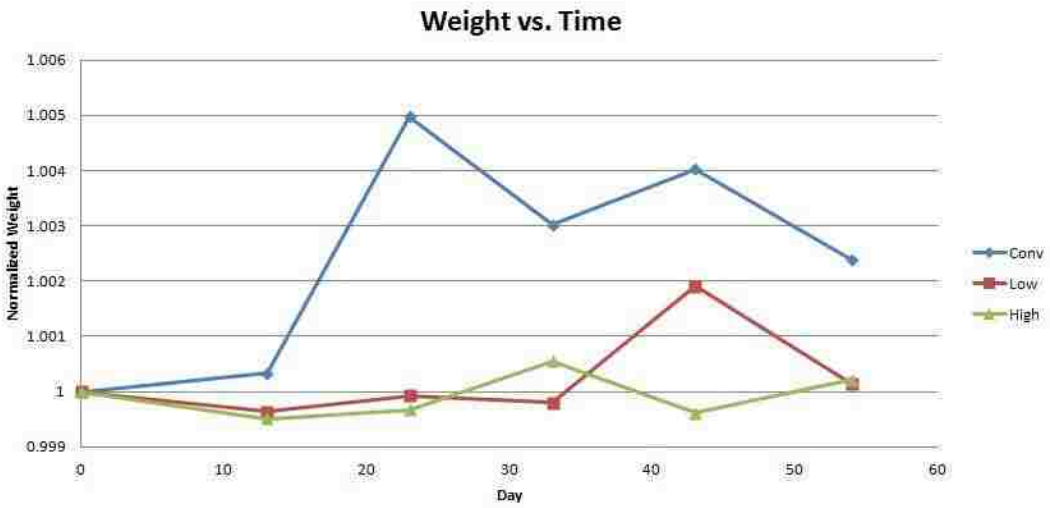

Figure 5.13: Mass vs. incubation time for enzymatic biodegradation

Unfortunately, the largest difference observed from the plots above was no greater than 4%. (The sudden decrease in week 18 of VAIM_Low sample of nonenzymatic biodegradation should be an error and it should not be taken into consideration in this research.) And it still needs to be further confirmed that whether these tiny changes should be considered as the real mass changes other than the noise influences.

5.6 Tensile Test Results and Discussion

Since orientation levels can affect the mechanical strength of dogbones, in the following section, comparisons of ultimate tensile strengths will be provided and discussed.

From Figures 5.14, 5.15 and 5.16, it is nice and clear to find that VAIM_High samples had the highest maximum load and ultimate stress from the beginning of the degradation, at least 5.3% higher than the conventional parts. And it remained as the highest level the most time during incubation, followed by the VAIM_Low and conventionally molded samples.

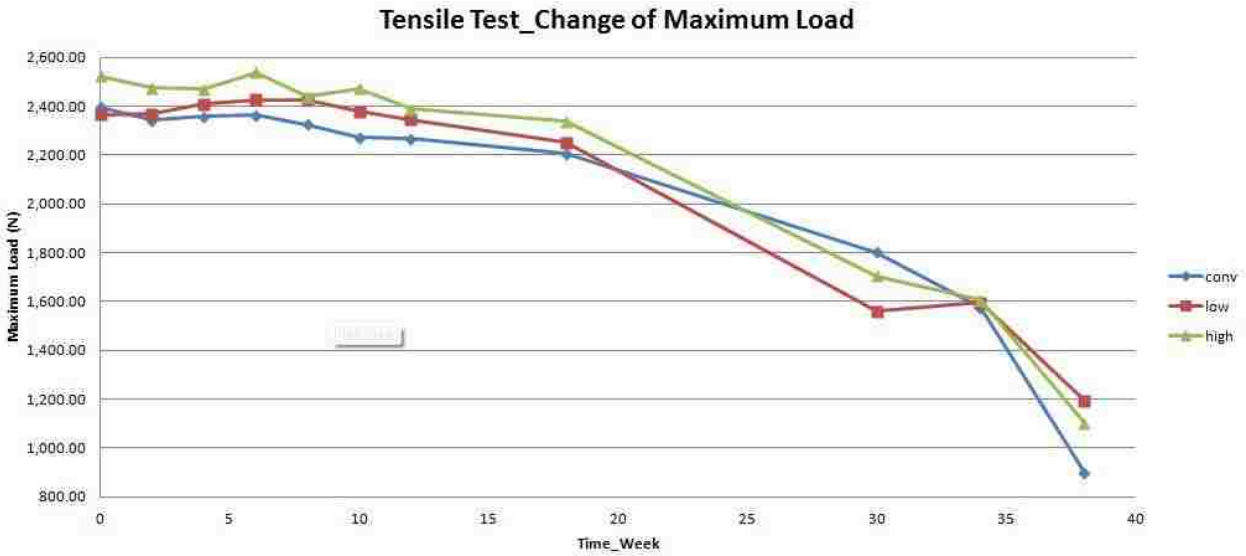

Figure 5.14: Maximum loads vs. incubation time for nonenzymatic biodegradation

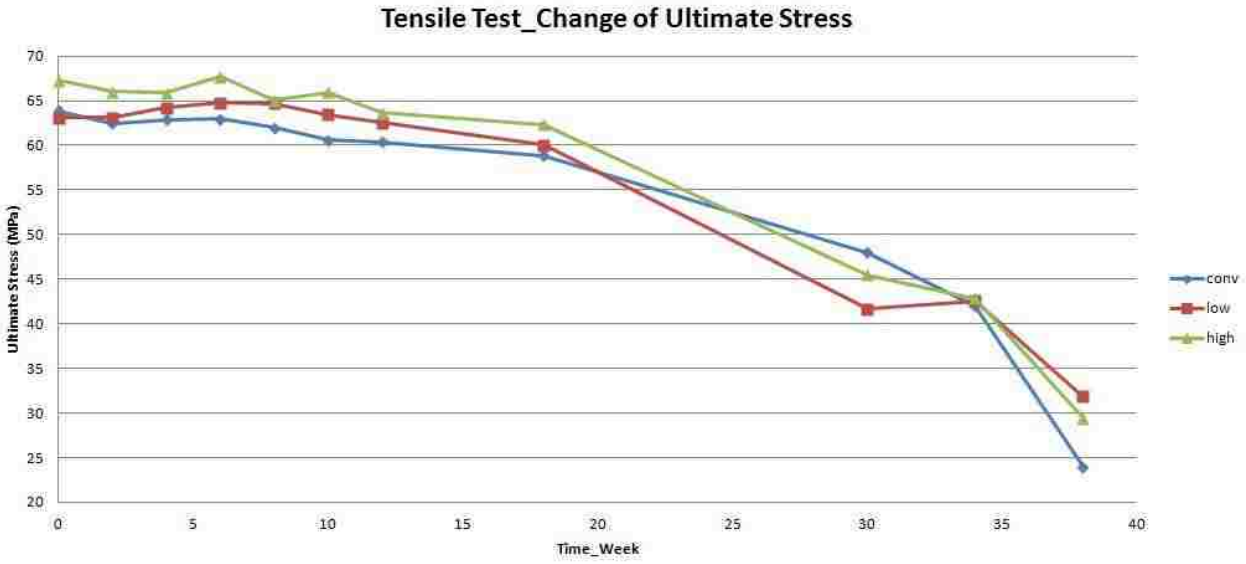

Figure 5.15: Ultimate stress vs. incubation time for nonenzymatic biodegradation

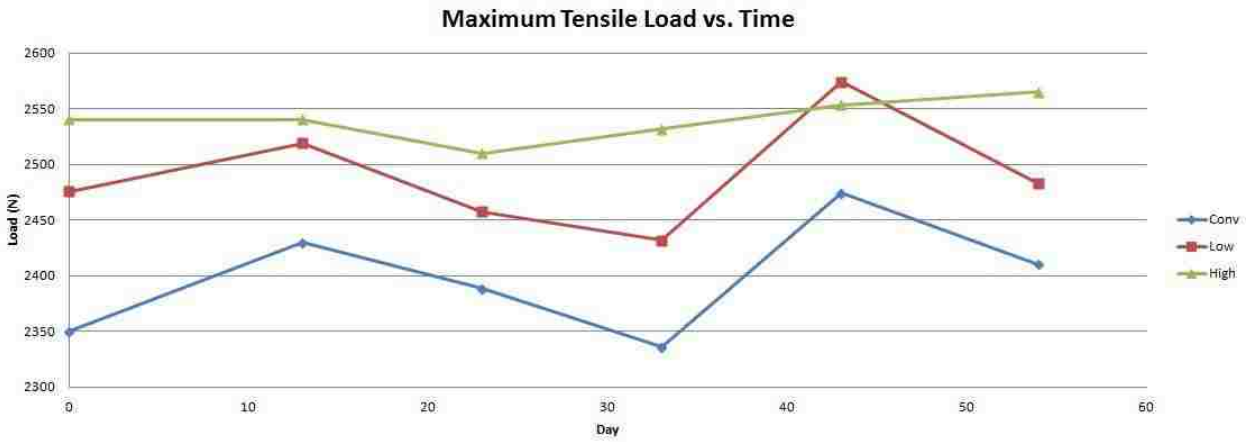

Figure 5.16: Maximum loads vs. incubation time for enzymatic biodegradation

For the enzymatic degradation (Figure 5.16), the maximum tensile loads of all types of samples acrually increased slightly over time, which was another unexpected result.

From all of the above, higher ultimate tensile load or stress can be achieved by applying a higher vibration frequency or duration, which can rearrange and toughen the inter-molecular forces in samples. So as hypothesized in Chapter 4, the increased level of the molecular orientation leads to the increased tensile strength parallel to the injection and vibration direction.

After months of study with all the six tests, though the experimental data and results could slightly differ from what was expected, there were still some remarkable results, which could present positive conclusions. These will be summarized in the final chapter.

Chapter 6: Conclusions and Recommendations

6.1 Conclusions

After several months of study of Vibration-Assisted Injection Molding (VAIM) and PLA biodegradation, some striking results and conclusions were clarified.

The molecular orientation of the polymer samples were successfully disturbed and rearranged by the VAIM technology. When cooled down to the room temperature, modified molecular orientation could be locked into the molded samples. (Figure 3.1) By applying different vibration frequencies and vibration durations, various degrees of molecular orientation were achieved. It was concluded that when molding the samples, the increase in vibration frequency or vibration duration was able to increase the molecular orientation level, which could be observed through the birefringence lamp. (Figure 3.8, Figure 3.9, Figure 3.10 and Figure 3.11) These molecular orientations inside the parts were also retained even after cutting, sanding or other trimming processes. (Figure 3.15)

VAIM and the associated molecular orientation was also able to change the biodegradation properties of PLA. Vibration-Assisted Injection Molding could break polymer chains. The long chains were shaken or vibrated during the molding, leading to some debondings along the polymer chains. So the highly oriented polymer samples had the relatively shorter molecule chains or smaller molecular weight initially. (Table 5.3)

During PLA biodegradation, though not perfectly, it was still clearly supported that molecular orientation can be a factor which influences the rate of

degradation as well as the temporal mechanical properties. Although there was not much significant result obtained in the weight measurement, the specimens with higher molecular orientation levels did possess more resistance against hydrolysis through the experimental tests. And tensile testing provided that VAIM_High dogbones had a tensile strength at least 5.3% higher than conventional ones.

GPC testing revealed normalized molecular weights of VAIM_High samples that were always higher than the normalized molecular weights of VAIM_Low samples. Even though the conventional samples had a higher normalized molecular weight than VAIM_Low parts at some times, it could be due to the fact that the initial molecular weight of conventionally molded samples was higher than the other two.

FT-IR testing revealed the fact that the infrared light absorption peak of hydroxyl groups for conventional specimens were always higher (or lower for transmittance peak in Figure 5.4 ~ Figure 5.7 actually) and the peak was growing faster than VAIM_Low and VAIM_High, indicating the hydrolysis occurred more readily in conventional samples.

Through DSC and TGA tests, degradation rates were investigated through the comparison of reductions of glass transition temperatures and onset temperatures of thermal degradation. It was clearly seen that the glass transition temperature of VAIM_High samples decreased the slowest and the Tg of conventional samples decreased the fastest. The onset temperature reduction rates showed a similar manner of Tg reduction. VAIM_High samples reduced the onset

temperature slower than VAIM_Low and conventional samples did. All results above meant that larger polymer molecules in conventional samples broke down to smaller ones faster than the other two types.

From the experimental data in enzymatic biodegradation, it could be indicated that the existance of proteinase K accelerated the biodegradation procedure, since some similar symptoms found in nonenzymatic biodegradation appeared earlier in the enzymatic biodegradation.

All the experimental results concluded that Vibration-Assisted Injection Molding was a convenient technology to produce large quantities of devices with different levels of molecular orientation for some types of thermolplastic materials. Also VAIM and the enzyme element (proteinase K in this study) could influence the biodegradation rate.

This technology may be applied in some medical areas as mentioned in Chapter 1 once the theory behind the phenomenon is fully developed. The shapes of molding samples can be determined by using different molds. The degradation rates of some medical implants can be predicted and specified just by using some combinations of VAIM molding factors and certain enzymes.

6.2 Recommendations For Future Work

Although there were some significant results and conclusions resulting from this research, recommendations and suggestions are still appropriate to advance this field further.

One limitation in this study may have been related to the VAIM process itself. Even though the increased vibration frequency and vibration duration increased the molecular orientation level in samples and made the samples more resistant against biodegradation, it was still not clear how frequency or duration affect the degradation rate individually.

There were also some unexpected or unknown results revealed through the data and plots of some applied tests denoted in Chapter 5. These include the growth of molecular weight in enzymatic incubation, no infrared light transmittance peak shifting of C-O bonds and C=O bonds over time, no significant changes in mass and the unexpected higher maximum loads in enzymatic degradation. Additionally, some other aspects, such as VAIM influence on the elongation and tensile modulus of products need to be investigated as well.

Further more, the frozen layer of the molded parts was ignored in this research. The frozen layer is neither completely the same as what results from conventional molding, nor similar to the VAIM molded core. It is this surface surface region that contacts the degradation environment first and may affect the biodegradation rate at the beginning. With this in mind, a future study could better take this into consideration.

Last, but not least, all experiments were based on just one kind of polymer with one type of enzyme. So in future tests, a wider range of biodegradable materials and enzymes should be listed in the research plan to widely and further prove the theory that VAIM induced molecular orientation can determine the biodegradation rate.

To sum up, for PLA specimens, Vibration-Assisted Injection Molding was able to tailor the molecular orientation level, which could influence the biodegradation rate remarkably, but all the improvements and recommendations mentioned above are necessary in deed, if any further investigation would be actualized.

Attachment I: Transmittance of The Infrared Light Corresponding to C-O Bond

Conventionally molded samples: (comparison among Week 0, 2, 6, 12, 18, 30,38)

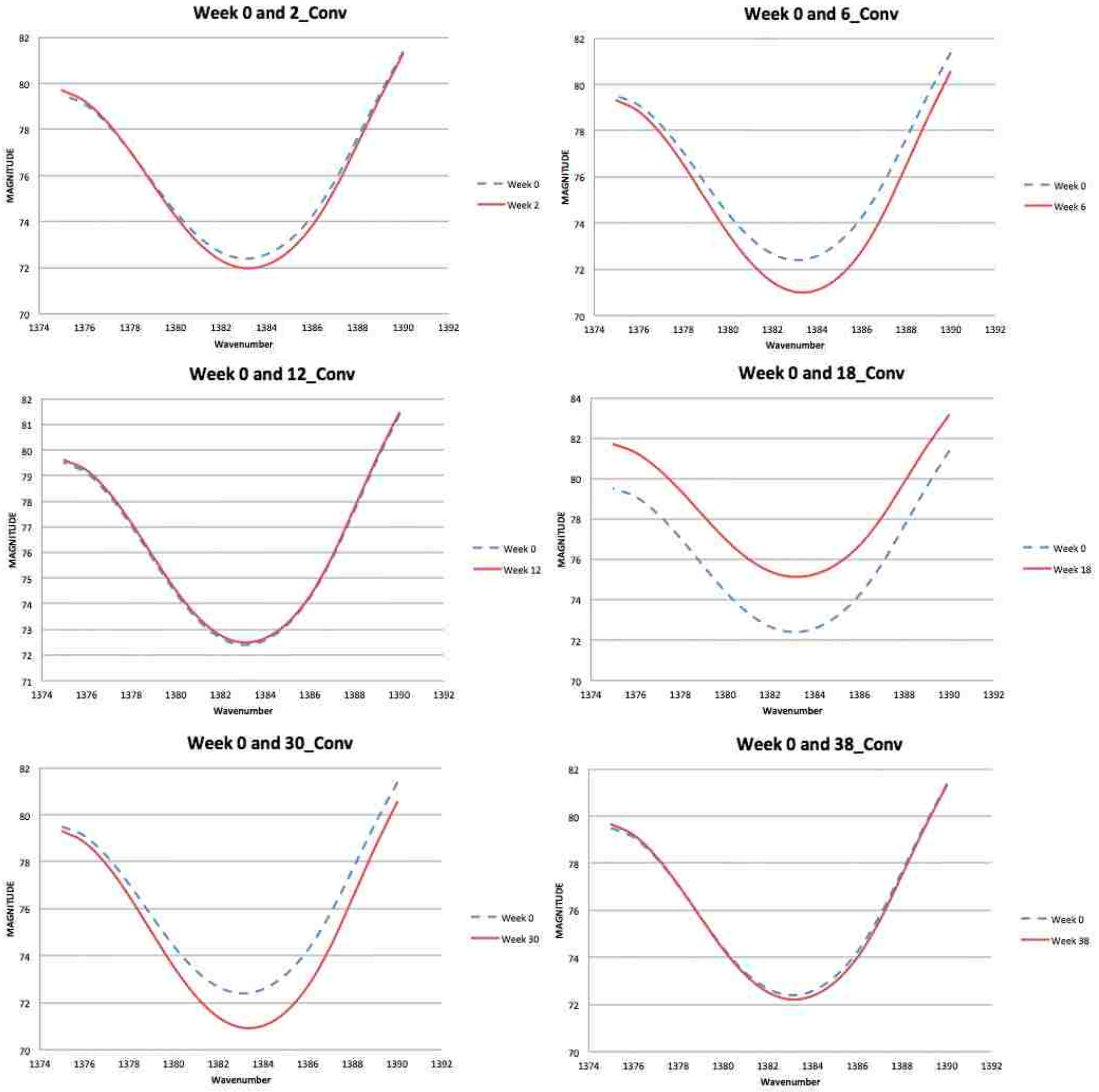

VAIM_Low molded samples: (comparison among Week 0, 2, 6, 12, 18, 30,38)

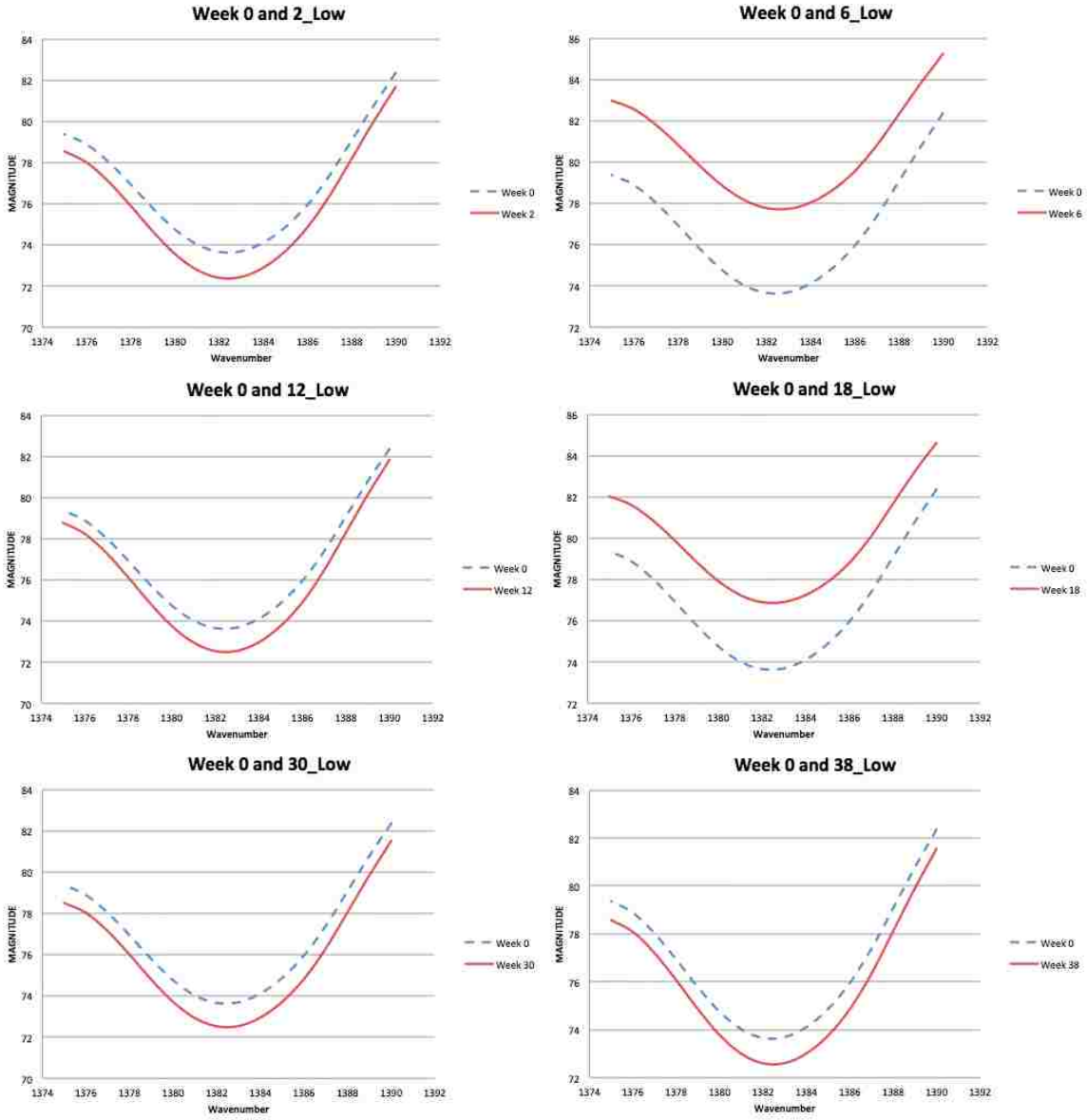

VAIM_High molded samples: (comparison among Week 0, 2, 6, 12, 18, 30,38)

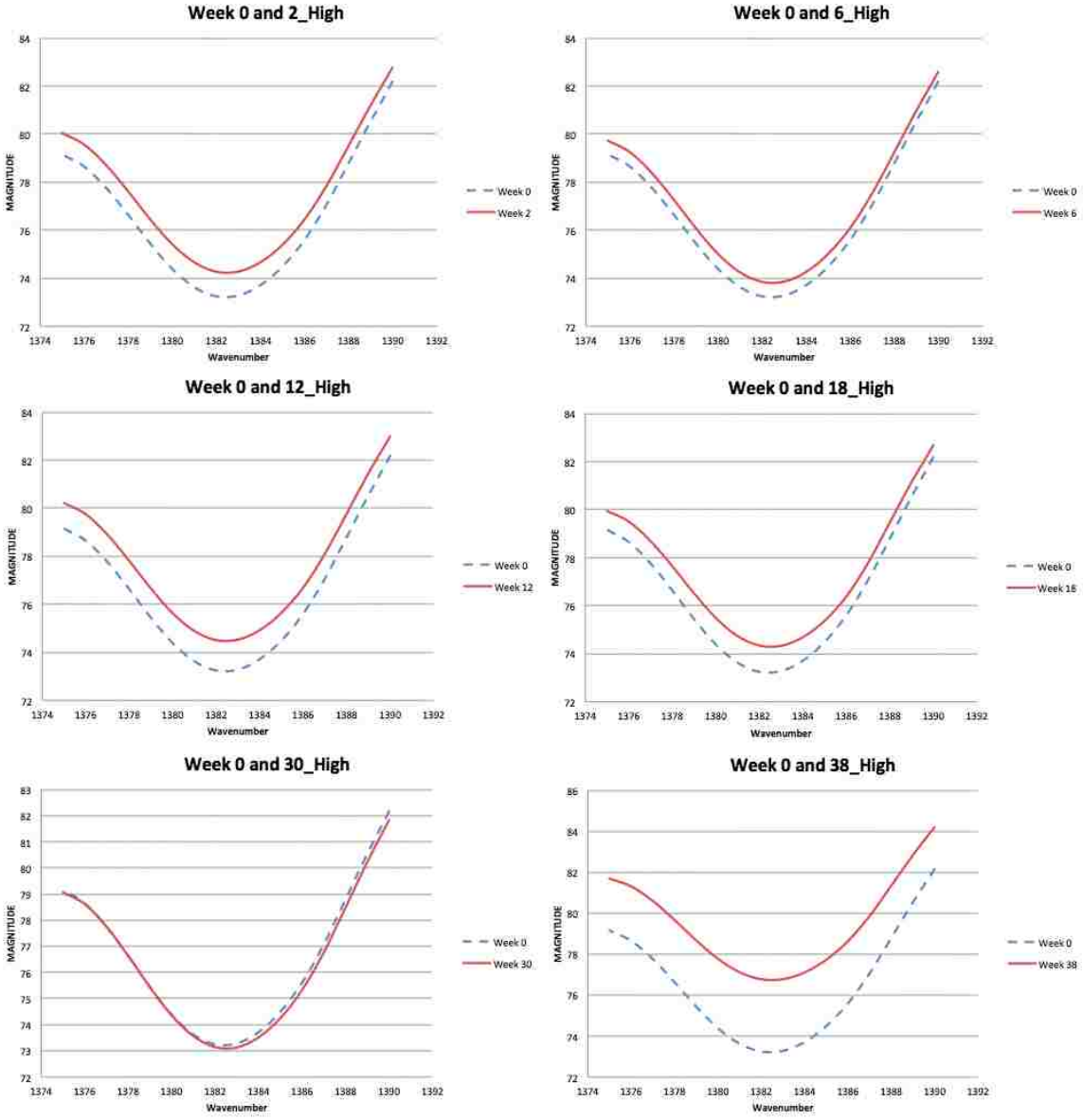

Attachment II: Transmittance of The Infrared Light Corresponding to C=O Bond

Conventionally molded samples: (comparison among Week 0, 2, 6, 12, 18, 30,38)

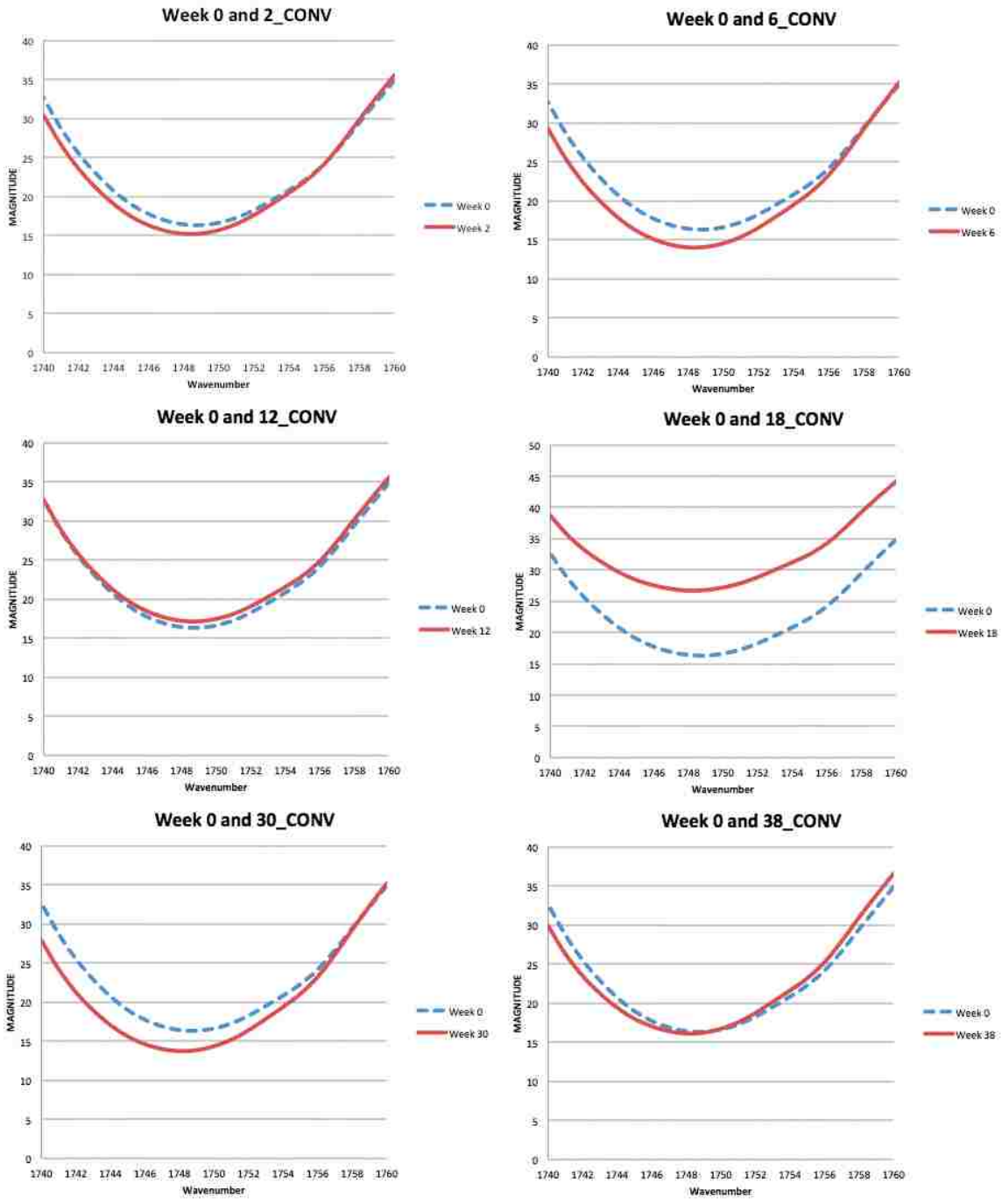

VAIM_Low molded samples: (comparison among Week 0, 2, 6, 12, 18, 30,38)

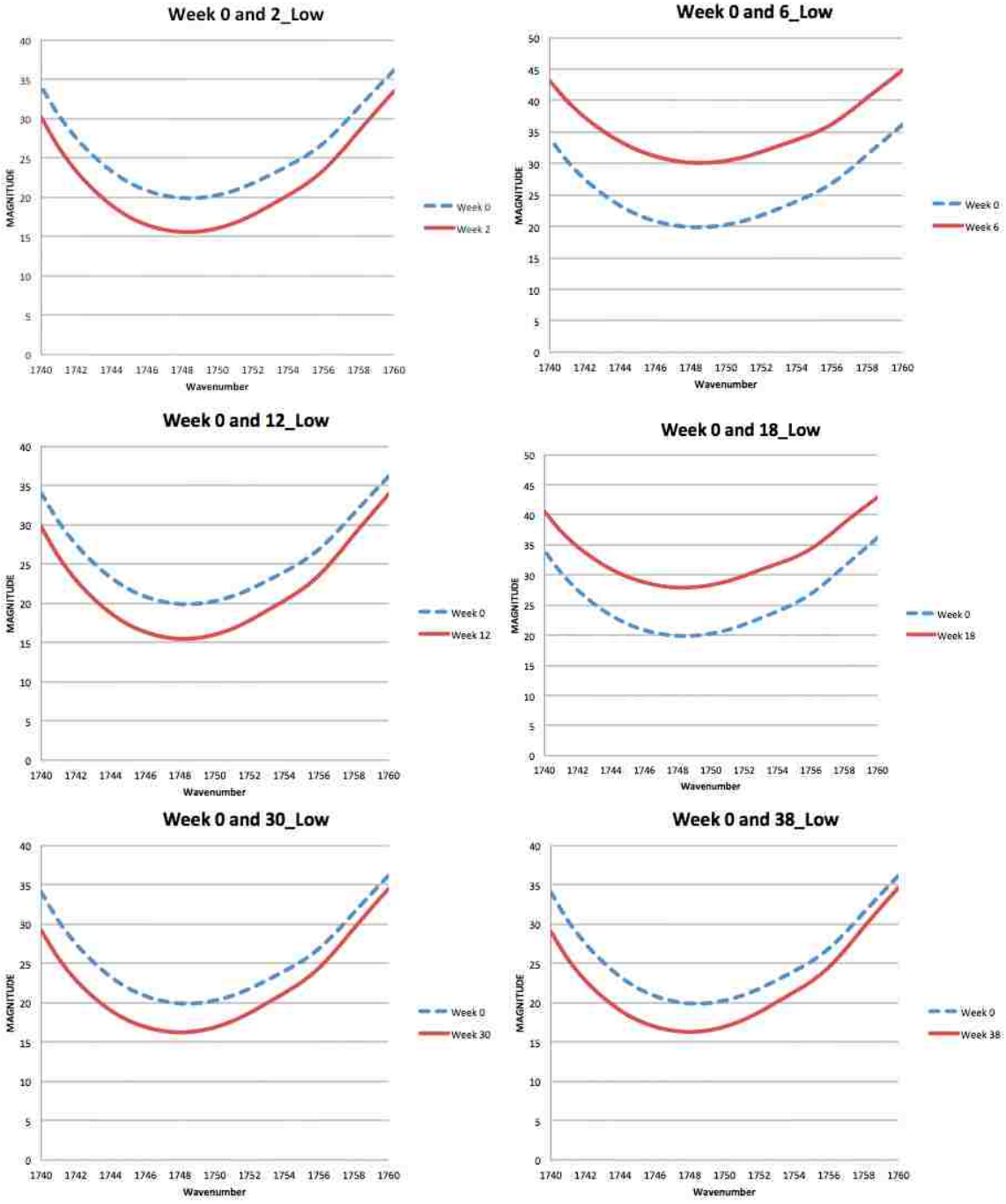

VAIM_High molded samples: (comparison among Week 0, 2, 6, 12, 18, 30,38)

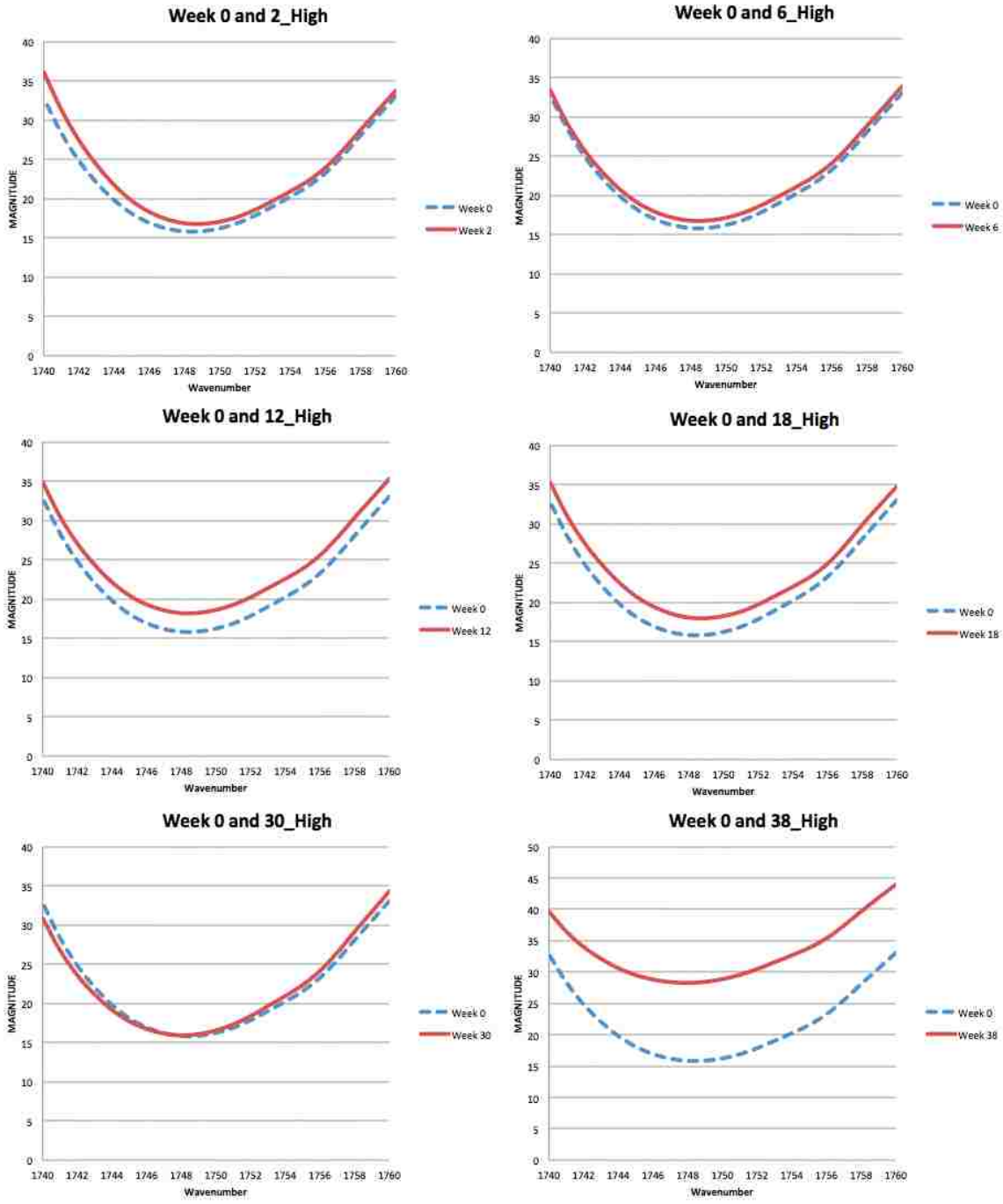

References:

[1]: Langer R, Peppas N. Chemical and physical structure of polymers as carriers for controlled release of bioactive agents: a review. J Macromol Sci-Rev A4acromol Chem Phys 1983; C23: 61-126.

[3]: GGpferich A, Langer R. Predicting drug release from cylindric polyanhydride matrix discs. Ellr J Pharmacol Biopharmacol1995; 41:81-87.

[4]: GGpferich A, Langer RS. Modeling of polymer erosion in three dimensions-Rotationally symmetric devices. AIChE J 1995; 41: 2292-2299.

[5]: D'Emanuele A, Hill J, Tamada A, Domb A, Langer R. Molecular weight changes in polymer erosion. Pharmacol Res 1992; 9: 1279-1283.

[6]: Laitinen O, Tormala P, Taurio R, Skutnabb K, Saarelainen K, Iivonen T, Vainionpaa S. Mechanical properties of biodegradable ligament augmentation device of poly(L-lactide) in vitro and in vivo. Biomaterials 1992; 13: 1012-1016.

[7]: Inion OY, Lääkärinkatu 2, FIN 33520, Tampere, Finland. An Introduction to Biodegradation Polymers as Implant Materials.

[8]: John C. Middleton, Arthur J. Tipton. Synthetic Biodegradable Polymers as Medical Devices. 1998.

[9]: Felix Simonovsky. University of Washington Engineered Biomaterials. Biomaterials Tutorial. 2004 <http://www.uweb.engr.washington.edu/research/tutorials/plagla.html>.

[10]: YTC America Inc. Biodegradable Plastics and Composites. <http://ytca.com/biodegradable_plastics_and_composites>.

[11]: <http://wire-spools.com/wooden-or-plastic-wire-spool-which-one-to-choose/>, <http://www.momgoesgreen.com/the-411-on-recycling-bottle-caps%E2%80%A6/>,

<http://innovationbazka.blogspot.com/2011_05_26_archive.html>,

<http://www.cachebeauty.com/Brushes/mini-hip_pocket_comb.htm>.

[12]: PLASTICS in wiki.

<http://plastics.inwiki.org/Image:Injection-molding-machine.gif>.

[13]: Gregory S. Layser. An Investigation of Controlled Melt-Manipulation Based Dynamic Injection-Molding Processes. Ph.D. Dissertation, Mechanical Engineering and Mechanics, Lehigh University, Bethlehem, PA, United States. Dec. 2007.

[14]: David C. Angstadt. An Investigation of Active Melt Manipulation During Polymer Processing And Its Effects on Part Mechanical Properties. Aug. 6, 2004.

[15]: Akihisa Kikushi. An Investigation of Vibration-Assisted Injection Molding for Enhanced Manufacturing. Jan. 2002.

[16]: Standard Test Method for Tensile Properties of Plastics, ASTM D638-2010.

[17]: Solutions for Molding Defects (Silver Streaks), Molding Defect Countermeasures, April15, 2011. <http://www.misumi-techcentral.com/tt/en/mold/2011/04/076-solutions-for-molding-defects-silver-streaks.html>.

[18]: NatureWork PLA Polymer 3051D Injection Molding Process Guide.

[19]: John W. Rodgers, AN INVESTIGATION OF THE EFFECTS OF DYNAMIC MELT CONTROL INJECTION MOLDING PROCESSES ON BIODEGRADABLE POLYMERS, 2010.

[20]: Odian G; Principles of Polymerization, 3rd ed., New York: John Wiley & Sons, 1991.

[21]: Osswald et al. International Plastics Handbook.. Munich: Hanser Publishers, 2006.

[22]: Yutaka Tokiwa, Buenaventurada P. Calabia, Charles U. Ugwu and Seiichi Aiba. Biodegradability of Plastics. International Journal of Molecular Sciences. 10, 3722-3742, 2009.

[23]: S. Li, M. Tenon, H. Garreau, C. Braud and M. Vert. Polymer Degradation Stability. 67 (2000) 85.

[24]: Suming Li, Inmaculada Molina, Manuel Bueno Martinez and Michel Vert. Hydrolytic and Enzymatic Degradations of Physically Crosslinked Hydrogels Prepared from PLA/PEO/PLA triblock copolymers. Journal of Materials Science: Materials in Medicine, 13(2002), 81-86.

[25]: Guarino V et al. Polylactic acid fiber-reinforced polycaprolactone scaffolds for bone tissue engineering. Biomaterials. 29(2008): 3662-3670.

[26]: Brian C. Smith. Fundamentals of Fourier Transform Infrared Spectroscopy. 1996.

[27]: G. W. H. Höhne, W. Hemminger and H. –J. flammersheim. Differential Scanning Calorimetry: An Introduction for Practitioners. 1995.

[28]: S. A. M. Ali, P. J. Doherty and D. F. Williams. Mechanisms of Polymer Degradation in Implantable Devices. 2. Poly(DL-lactic acid). Journal of Biomedical Materials Research, Vol. 27, 1409-1418 (1993).

[29]: Clément Duval. Inorganic Thermogravimetric Analysis. 1963.

[30]: Krzysztof Pielichowski, James Njuguna. Thermal Degradation of Polymeric Materials. 2005.

[31]: <http://www.absoluteastronomy.com/topics/Infrared_spectroscopy>.

VITA:

Qi Li was born on May 4th, 1987 to Jiangang Li and Sufang Wen. He grew up in Taiyuan, Shanxi Province in China. He received his B.S. degree in Mechanical Engineering from Beihang University, Beijing, in 2009. In the same year, he was accepted by Lehigh University as a master student. Upon completing his Master's degree in Mechanical Engineering and Mechanics, he is planning to continue pursuing his Ph.D. in the same department at Lehigh University.